THE ASTROPHYSICAL JOURNAL, 348:682–699, 1990 January 10


# PHOTOMETRIC AND SPECTROSCOPIC MODELING OF STARSPOTS ON THE RS CANUM VENATICORUM BINARY HD 26337

KLAUS G. STRASSMEIER[1]
Department of Physics and Astronomy, Vanderbilt University, and Center of Excellence in Information Systems Engineering, Tennessee State University
*Received 1988 December 21; accepted 1989 July 11*

## ABSTRACT

A photometric and spectroscopic study has been conducted of the rapidly rotating G5 subgiant in the single-lined RS CVn binary HD 26337 (=EI Eri). This included partially simultaneous observations of active chromosphere and photosphere characteristics. High-resolution line profiles are used for starspot modeling with the Doppler imaging technique, while simultaneous *VRI* photometry is used for light and color curve spot modeling. The long-term behavior of the cool starspot regions has been studied by light curve modeling of 9 years of *V*-band photometry.

The Doppler imaging solution yielded a polar spot and a number of smaller spots close to or even touching the polar spot. The existence of a polar spot is rather well determined from spectroscopy and photometry and agrees with results for the spotted stars HR 1099 and HD 199178 obtained by Vogt and collaborators. Our light curve solution derived from simultaneous photometry is qualitatively consistent with the Doppler imaging results, but it has incorrectly low latitudes.

Our photometry also detected very rapid light curve changes on a time scale of only one or two rotation cycles which are presumably due to intrinsic spot variability. A long-term variability of the mean light level is also present. Some evidence for differential rotation with longitude migration rates 10 times smaller than on the Sun appears as well. We suggest tentatively that the combined effects of a strong meridional plasma flow and differential rotation cause the short-lived equator spots and also cause the long-lived polar spot.

*Subject headings:* line profiles — photometry — stars: binaries — stars: individual (HD 26337)

## I. INTRODUCTION

The strong Ca II H and K emission of HD 26337 (=EI Eri, $V \approx 7.0$ mag, spectral type G5 IV) has been detected by Bidelman and MacConnell (1973), but it took another 10 years to discover its light variability and consequently to classify the star as a RS CVn binary (Fekel *et al.* 1982). Subsequently, Fekel *et al.* (1987) computed an orbit for this single-lined spectroscopic binary with a period of 1.94722 days, while Hall *et al.* (1987) found a *rotation* period of 1.945 days from *UBV* photometry and concluded that the G5 IV component in HD 26337 rotates synchronously. The star has been detected at radio frequencies (Mutel and Lestrade 1985), at microwave frequencies (Slee *et al.* 1988), and in the infrared at 12 $\mu$m (Busso *et al.* 1988), and has strong ultraviolet emission lines (Fekel *et al.* 1987) typical of chromospherically active stars. No X-ray observations are available to date.

In recent years, spot modeling of multicolor light curves has become a common tool for the starspot researcher. This technique, however, suffers from ambiguity problems of the many free parameters. With reasonable assumptions, it reproduces the spot's longitude, area, and temperature very well, but it generally fails to give unambiguous information about the spot's latitude and shape.

The large projected rotational velocity of HD 26337 of 50 km $s^{-1}$ (Fekel, Moffett, and Henry 1986), the intermediate inclination of the rotation axis of 46° (Fekel *et al.* 1987), and the observed light variability presumably due to cool starspots make HD 26337 a good candidate for the Doppler imaging technique (Vogt and Penrod 1983). This technique allows the reconstruction of the surface brightness distribution of a rapidly rotating star by analysis of distortions in the line profiles and hence includes information of the spot latitude. Only a few Doppler maps of spotted stars have been published so far: three for HR 1099 (Vogt and Penrod 1983; Vogt 1988) and one for HD 199178 (Vogt 1988). The particular problems with this technique are the stringent signal-to-noise ratio and resolution requirements, the good phase coverage, and the complexity of the analysis software. In the case of HD 26337, we have an additional problem: the rotation period is only slightly shorter than exactly 2.0 days, so that it takes an observer at least 20 nights to cover a full rotation cycle. Moreover, Hall *et al.* (1987) noted month-to-month changes in the light curves in 1985 which restrict the total time span for the Doppler imaging observations to one month.

A striking feature of *all* previous Doppler images is the long-lived polar spot which suggests that magnetic activity on very rapidly rotating stars can be qualitatively different from that seen on the Sun (Vogt 1988). Therefore, it seems crucial for a future successful formulation of a dynamo theory for rapidly rotating chromospherically active stars to manifest (or contradict) these polar spots. By applying both spot modeling techniques, viz., light curve modeling and Doppler imaging, to *simultaneous* observations, we may also check the capabilities and restrictions of each method. Strassmeier (1987) initiated an international campaign of simultaneous multicolor photometry and Doppler imaging of HD 26337 which is still going on. In this paper, we report the observations made in the 1987–1988 observing season and apply the light and color curve modeling technique (§ VI) to the data obtained. In § VII, we

[1] Visiting astronomer, Kitt Peak National Observatory and Kitt Peak National Solar Observatory, operated by the Association of Universities for Research in Astronomy, Inc., under contract with the National Science Foundation.

investigate the long-term spot behavior from 9 years of $V$-band photometry.

## II. INSTRUMENTATION

### a) Photometry

The 1987–1988 observing season photometry was obtained by several observers (Hooten *et al.* 1989) at different observatories in the United States, Europe, Japan, and South America, and by the 0.4 m Vanderbilt automatic photoelectric telescope (APT) on Mount Hopkins, Arizona. The Vanderbilt APT utilized a thermoelectrically cooled GaAs Hamamatsu R943-02 photomultiplier tube with filters which were selected to match *UBV* of the Johnson system and *RI* of the Kron-Cousins system. G. Cutispoto, at the European Southern Observatory (ESO), Chile, used standard ESO pulse-counting equipment and filters which matched *UBV* of Johnson and *RI* of Kron-Cousins. O. Oshima, at the Tamashima Observatory, Japan, used a Hamamatsu R647-04 photomultiplier tube, while Y. Ito at the Kakuda Joshi Observatory, also in Japan, used an RCA 1P21 tube. S. Englebrektson and M. Ganis used an EMI Gencom photometer. All other observatories listed in Table 1 utilized an Optec SSP-3 solid-state photometer with filters to match the Johnson *UBVRI* system. A journal of the observers, the observatories, and the number of measures in each passband are given in Table 1. The new 1986–1987 observing season light curve (labeled "1987.12" in Fig. 10*d*) has been obtained with the 0.25 m Phoenix APT (Boyd, Genet, and Hall 1984), also located on Mount Hopkins, which utilized an unrefrigerated 1P21 photomultiplier and filters to match the Johnson *UBV* system.

### b) Spectroscopy

The red wavelength high-resolution line-profile observations were carried out with the Kitt Peak National Observatory's (KPNO) 0.9 m coudé feed telescope and the National Solar Observatory's (NSO) McMath solar telescope equipped with the stellar spectrograph.

The coudé feed spectra were obtained in three different spectrograph-detector combinations: camera 6, grating B, and TI-3 CCD; camera 6, grating A, and TEK-CCD; Camera 5, grating A, and TI-3 CCD. The MacMath spectra were taken with the B & L grating I, 105 mm transfer lens, and TI-4 CCD. The instrumental resolution achieved varied between 35,000 and 45,000, with signal-to-noise ratios (S/N ratio) of 135–450. The individual observations, their integration time, dispersion, resolution, S/N ratio, wavelength field, and telescope-detector configuration are listed in Table 2. An example of the data along with a comparison of the different wavelength fields of the various telescope-spectrograph-detector combinations is shown in Figure 1.

Simultaneous with the red wavelength observations, we obtained blue spectra which included the Ca II H and K emis-

TABLE 1

JOURNAL OF PHOTOMETRIC OBSERVATIONS

| Observer[a] | Location | Telescope Aperture (cm) | *U* | | *B* | | *V* | | *R* | | *I* | |
|---|---|---|---|---|---|---|---|---|---|---|---|---|
| | | | *m* | *n* | *m* | *n* | *m* | *n* | *m* | *n* | *m* | *n* |
| ... ..... | APT, Mount Hopkins, Tucson, AZ | 40 | 4 | 62 | 4 | 60 | 4 | 59 | 4 | 64 | 4 | 63 |
| Barksdale ..... | Barksdale Observatory Winter Park, FL | 35 | ... | ... | ... | ... | 6 | 63 | 6 | 59 | 5 | 54 |
| Bertoglio ..... | Cuneo Observatory, Torino, Italy | 20 | ... | ... | ... | ... | 2 | 10 | ... | ... | 2 | 10 |
| Cortesi ..... | Specola Solare Ticinese, Locarno, Switzerland | 50 | ... | ... | 11 | 30 | 11 | 30 | 11 | 30 | 11 | 30 |
| Cutispoto ..... | European Southern Observatory, La Silla, Chile | 50 | 13 | 13 | 13 | 13 | 13 | 13 | 13 | 13 | 13 | 13 |
| Engelbrektson ... Ganis | Pace University Observatory, NY | 28 | ... | ... | ... | ... | 9 | 63 | ... | ... | ... | ... |
| Gómez, Casas ... Gallart, Jariod | Grup d'Estudis Astronomics; Barcelona, Spain | 20, 30, 41 | ... | ... | ... | ... | 7 | 10 | 2 | 2 | 1 | 1 |
| Melillo ..... | Valley Stream Observatory, Valley Stream, NY | 20 | ... | ... | ... | ... | 2 | 2 | ... | ... | 2 | 2 |
| Ito ..... | Kakuda Joshi Observatory Kakuda, Japan | 15 | ... | ... | 2 | 31 | 2 | 39 | ... | ... | ... | ... |
| Ohshima ..... | Tamashima Observatory Kurashiki, Japan | 20 | 12 | 500 | 12 | 500 | 12 | 500 | ... | ... | ... | ... |
| Poole ..... McLaughlin | Grant Observatory, Pittsburgh, PA | 25 | ... | ... | ... | ... | 1 | 5 | 1 | 5 | 1 | 5 |
| Powell, Nix ..... | East Tennessee State University Johnson City, TN | 20 | ... | ... | ... | ... | 3 | 13 | 3 | 13 | 3 | 13 |
| Soder ..... | Einstein Astrophysical Observatory Sidney, OH | 20 | ... | ... | ... | ... | 1 | 3 | 1 | 3 | 1 | 3 |
| Wasson ..... | Sunset Hills Observatory Hacienda Heights, CA | 35 | ... | ... | ... | ... | 2 | 8 | ... | ... | ... | ... |

NOTE.—*m* is the number of nights on which HD 26337 was observed; *n* is the total number of individual measurements and is not necessarily an average value.

[a] Hooten *et al.* 1989.

TABLE 2

JOURNAL OF SPECTROSCOPIC OBSERVATIONS

| Number | $\phi_{rot}$ | HJD of mid-Exposure (244+) | Integration Time (min) | Reciprocal Dispersion (Å mm$^{-1}$) | Effective Resolution (Å) | Wavelength Coverage (Å) | S/N Ratio | Telescope-Detector Combination[a] |
|---|---|---|---|---|---|---|---|---|
| Red Wavelength Observations | | | | | | | | |
| 1 ..... | 0.044 | 7152.5664 | 70 | 7 | 0.15 | 6388–6472 | 200 | CF5, TI-3 |
| 2 ..... | 0.068 | 7150.6665 | 90 | 4.2 | 0.18 | 6400–6450 | 170 | CF6, TI-3 |
| 3 ..... | 0.100 | 7150.7295 | 90 | 4.2 | 0.18 | 6400–6450 | 160 | CF6, TI-3 |
| 4 ..... | 0.128 | 7152.7280 | 90 | 7 | 0.15 | 6388–6472 | 250 | CF5, TI-3 |
| 5 ..... | 0.134 | 7150.7964 | 90 | 4.2 | 0.18 | 6400–6450 | 160 | CF6, TI-3 |
| 6 ..... | 0.201 | 7150.9253 | 82 | 4.2 | 0.18 | 6400–6450 | 140 | CF6, TI-3 |
| 7 ..... | 0.279 | 7156.9126 | 75 | 2.0 | 0.18 | 6420–6450 | 135 | CF6, TEK |
| 8 ..... | 0.399 | 7170.7617 | 60 | 6.4 | 0.14 | 6408–6484 | 450 | McM, TI-4 |
| 9 ..... | 0.467 | 7170.8936 | 60 | 6.4 | 0.17 | 6408–6484 | 350 | McM, TI-4 |
| 10 ..... | 0.538 | 7151.5811 | 60 | 7 | 0.15 | 6388–6472 | 200 | CF5, TI-3 |
| 11 ..... | 0.625 | 7151.7505 | 60 | 7 | 0.15 | 6388–6472 | 220 | CF5, TI-3 |
| 12 ..... | 0.628 | 7157.5918 | 90 | 2.0 | 0.18 | 6420–6450 | 170 | CF6, TEK |
| 13 ..... | 0.664 | 7157.6611 | 83 | 2.0 | 0.18 | 6420–6450 | 150 | CF6, TEK |
| 14 ..... | 0.698 | 7158.8926 | 60 | 7 | 0.15 | 6388–6472 | 190 | CF5, TI-3 |
| 15 ..... | 0.742 | 7157.8130 | 90 | 2.0 | 0.18 | 6420–6450 | 240 | CF6, TEK |
| 16[b] ..... | 0.756 | 7163.6748 | 5 | 6.4 | 0.15 | 6400–6476 | 80 | McM, TI-4 |
| 17 ..... | 0.769 | 7163.6997 | 60 | 6.4 | 0.15 | 6400–6476 | 400 | McM, TI-4 |
| 18 ..... | 0.788 | 7157.9033 | 90 | 2.0 | 0.18 | 6420–6450 | 220 | CF6, TEK |
| 19 ..... | 0.792 | 7163.7451 | 60 | 6.4 | 0.15 | 6400–6476 | 350 | McM, TI-4 |
| 20[b] ..... | 0.816 | 7163.7920 | 5 | 6.4 | 0.15 | 6408–6484 | 80 | McM, TI-4 |
| 21 ..... | 0.827 | 7163.8130 | 50 | 6.4 | 0.15 | 6408–6484 | 300 | McM, TI-4 |
| 22 ..... | 0.845 | 7163.8486 | 50 | 6.4 | 0.15 | 6408–6484 | 340 | McM, TI-4 |
| 23 ..... | 0.865 | 7163.8882 | 60 | 6.4 | 0.15 | 6508–6484 | 330 | McM, TI-4 |
| Blue Spectra (including Ca II H and K emission lines) | | | | | | | | |
| 1[c] ..... | 0.034 | 7142.8208 | 40 | 15 | 0.5 | 3900–4350 | 100 | DAO, RET |
| 2 ..... | 0.145 | 7158.5972 | 60 | 4.7 | 0.24 | 3920–3984 | 150 | CF5, TEK |
| 3 ..... | 0.215 | 7158.7340 | 60 | 4.7 | 0.24 | 3920–3984 | 250 | CF5, TEK |
| 4[c] ..... | 0.510 | 7141.8018 | 33 | 15 | 0.5 | 3900–4350 | 100 | DAO, RET |

[a] CF6, TI-3: coudé feed with camera No. 6, grating B, TI-3 CCD. CF6, TEK: coudé feed with camera No. 6, grating A, TEK CCD. CF5, TI-3: coudé feed with camera No. 5, grating A, TI-3 CCD. McM, TI-4: McMath Solar Telescope, stellar spectrograph, B & L grating I, 105 mm transfer lens, TI-4 CCD. CF5, TEK: coudé feed with camera No. 5, grating A, TEK CCD. DAO, RET: Dominion Astrophysical Observatory 1.8 m Cassegrain with 1872 pixel Reticon.

[b] Not used in the Doppler imaging analysis.

[c] Provided by B. W. Bopp, DAO.

sion lines (Table 2). The KPNO coudé feed telescope was used with camera 5, grating A, and the TEK-CCD; the larger slit width compared to the red observations gave a resolution of 16,000 at Ca II. I am indebted to B. W. Bopp for providing me with two additional H and K observations made at the Dominion Astrophysical Observatory (DAO) simultaneous with the other observations (Table 2).

## III. ORBIT

To permit accurate removal of orbital radial velocity variations from the line profiles, we first recomputed the orbital elements with our new radial velocities and then shifted the individual line profiles according to their theoretical value. The new radial velocities presented in Table 3 were determined relative to one of the following velocity standards: $\beta$ Gem ($+3.3$ km s$^{-1}$), $\alpha$ Ari ($-14.3$ km s$^{-1}$), 10 Tau ($+27.9$ km s$^{-1}$), and $\iota$ Psc ($+5.3$ km s$^{-1}$), or relative to atmospheric water vapor lines. If a standard star observation was available we have used a cross-correlation program written at KPNO (Willmarth and Abt 1985).

The observations presented in this paper, combined with data obtained earlier by Fekel *et al.* (1987), are plotted in Figure 2 along with the computed radial velocity curve. We adopted Fekel *et al.*'s orbit as our starting solution and computed final elements from the combined data set using the differential correction program of Barker, Evans, and Laing (1967). The formal solution gave a value for the eccentricity of $0.011 \pm 0.012$, so in accordance with Fekel *et al.* (1987) and the precepts of Lucy and Sweeny (1971), an $e = 0$ solution has been adopted. Table 4 lists the improved orbital elements for the combined data set ("This Paper") and Fekel *et al.*'s (1987) elements.

## IV. CHROMOSPHERIC EMISSION

### a) *Absolute* Ca II H *and* K *Fluxes*

The absolute surface flux measurements of the Ca II H and K emission lines in ergs cm$^{-2}$ s$^{-1}$ followed the procedure described by Linsky *et al.* (1979). Table 5 lists the measured fluxes for the four available spectra: log $\mathcal{F}$(H) and log $\mathcal{F}$(K) are the observed fluxes, while log $\mathcal{F}'$(H) and log $\mathcal{F}'$(K) are the radiative losses in the H and K lines, respectively, that is, the net chromospheric flux after subtraction of the flux which arises from the underlaying photosphere. Comparison with fluxes from other G5 subgiants shows HD 26337 to be a very chromospherically active system, having a net radiative loss in

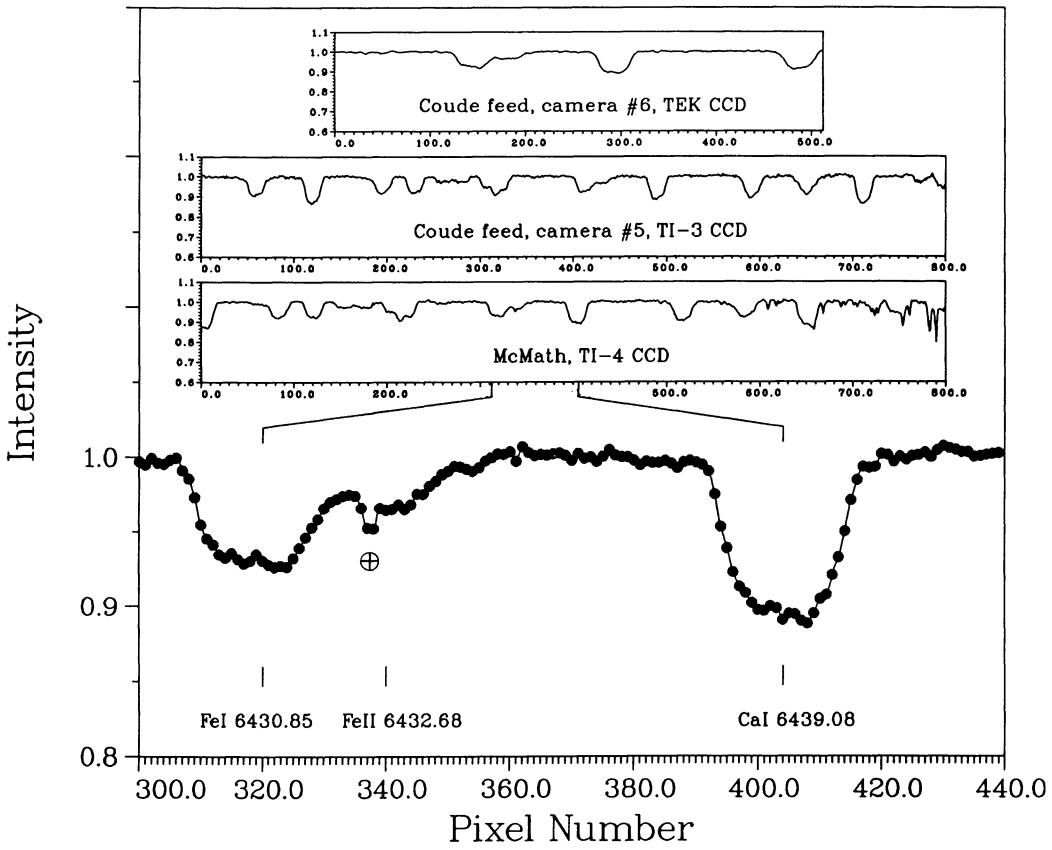


FIG. 1.—Example of raw data. Full wavelength range for the various instrument combinations is shown in the inset graphs. Main graph is an enlargement of the Fe I 6430 Å and Ca I 6439 Å line region from the NSO McMath spectrum shown in the lower inset. Resolution in this spectrum is 0.15 Å corresponding to two pixels.

TABLE 3

NEW RADIAL VELOCITIES OF HD 26337

| HJD (2,440,000+) | Orbital Phase[a] | $v$ (km s$^{-1}$) | O − C (km s$^{-1}$) | Standard | Code[b] |
|---|---|---|---|---|---|
| 7150.6665..... | 0.728 | 13.1 | −0.1 | β Gem | CF6, TI-3 |
| 7150.7295..... | 0.760 | 19.3 | 0.5 | β Gem | CF6, TI-3 |
| 7150.7964..... | 0.795 | 25.0 | 0.3 | β Gem | CF6, TI-3 |
| 7150.9253..... | 0.861 | 32.7 | −2.0 | β Gem | CF6, TI-3 |
| 7151.5811..... | 0.197 | 27.0 | −0.3 | ι Psc | CF5, TI-3 |
| 7151.7505..... | 0.284 | 14.4 | 1.6 | α Ari | CF5, TI-3 |
| 7151.8926..... | 0.357 | 2.4 | 1.1 | 10 Tau | CF5, TI-3 |
| 7152.5664..... | 0.704 | 10.2 | 1.1 | α Ari | CF5, TI-3 |
| 7152.7280..... | 0.787 | 22.9 | −0.4 | 10 Tau | CF5, TI-3 |
| 7156.9126..... | 0.935 | 42.4 | 0.1 | β Gem | CF6, TEK |
| 7157.5918..... | 0.284 | 12.7 | −0.1 | α Ari | CF6, TEK |
| 7157.6611..... | 0.320 | 5.7 | −1.2 | α Ari | CF6, TEK |
| 7157.8130..... | 0.398 | −3.0 | 0.8 | α Ari | CF6, TEK |
| 7157.9033..... | 0.444 | −6.4 | 1.6 | β Gem | CF6, TEK |
| 7163.6997..... | 0.421 | −10.2 | −4.1 | $H_2O$ | McM, TI-4 |
| 7163.7451..... | 0.444 | −6.0 | 2.0 | $H_2O$ | McM, TI-4 |
| 7163.8130..... | 0.479 | −10.8 | −1.1 | β Gem | McM, TI-4 |
| 7163.8486..... | 0.498 | −10.8 | −0.8 | β Gem | McM, TI-4 |
| 7163.8882..... | 0.518 | −11.0 | −1.0 | β Gem | McM, TI-4 |
| 7170.7617..... | 0.048 | 43.0 | −0.7 | $H_2O$ | McM, TI-4 |
| 7170.8936..... | 0.115 | 38.5 | 0.1 | $H_2O$ | McM, TI-4 |

[a] Computed with the elements HJD 2,446,074.384 + 1.94722$E$.
[b] See Table 2.

the H and K lines of $\mathcal{F}'(H + K) = 9.7 \times 10^6$ ergs cm$^{-2}$ s$^{-1}$, similar to HD 31738 and HD 12545, two other spectroscopic binaries containing a G5 subgiant, but over 30 times that of the "inactive" single G5 subgiant $\mu$ Her A. Figure 3 is an example of a KPNO coudé feed scan showing the strong H and K emission lines with equivalent widths (measured relative to the pseudo continuum) of 0.352 and 0.620 Å, respectively. Only one-half of a rotation cycle has been covered; thus, no definite statement with respect to rotational flux modulation can be made. However, we may point out that the flux at rotation phase 0.034 (Table 5) is about 50% larger than that at phase 0.510 measured the night before.

### *b*) H$\alpha$ *Core Emission*

We have used older H$\alpha$ spectra of HD 26337 obtained on four consecutive nights in 1983 August by G. W. Henry at McDonald Observatory, and presented in Fekel, Moffett, and Henry (1986), to derive a more quantitative measure of chromospheric activity displayed in the Balmer H$\alpha$ line. Figure 11 in Fekel, Moffett, and Henry (1986) is a plot of the H$\alpha$ region of HD 26337 and shows a very weak, almost absent, absorption feature, which turned out to be quite variable also.

Using the H$\alpha$ profile of the single nonactive G5 subgiant $\mu$ Her A ($W_{H\alpha} = -1.078 \pm 0.025$ Å; observed with the same configuration and artificially broadened to $v \sin i = 50$ km s$^{-1}$) as a reference, and subtracting this profile from each of the HD 26337 scans, we measured core-emission equivalent widths of +0.990, +0.484, +0.960, and +0.815 Å at rotation phases of 0.378, 0.889, 0.397, and 0.920, respectively. Thus, rotational

TABLE 4

IMPROVED ORBITAL ELEMENTS

| Elements | This Paper | Fekel *et al.* (1987) |
|---|---|---|
| Period (days) | 1.947227±0.000008 (m.e.) | 1.94722±0.00003 (m.e.) |
| $T_0$ (HJD) | 2,446,091.052 | 2,446,074.384 |
| $\gamma$ (km s$^{-1}$) | 17.6±0.2 | 17.6±0.4 |
| $K_1$ (km s$^{-1}$) | 27.4±0.3 | 27.2±0.6 |
| $e$ (assumed) | 0.0 | 0.0 |
| $a_1 \sin i$ ($10^5$ km) | 7.33±0.09 | 7.29±0.16 |
| $f(M)(M_\odot)$ | 0.00415±0.00015 | 0.0041±0.00027 |
| Standard error of an observation of unit weight | 1.6 km s$^{-1}$ | 1.6 km s$^{-1}$ |

modulation of the chromospheric emission at Hα seems to be present, presumably due to (changing) plage regions on the stellar surface moving in and out of view.

## V. LIGHT CURVE MODELING OF THE SIMULTANEOUS PHOTOMETRY

### *a) The Observations*

The individual measurements were made differentially with respect to 37 Eri ($V = 5.44$ mag, $B = 6.38$ mag; Nicolet 1978), except for those of G. Cutispoto at ESO, who used HD 25852 as the comparison star. The standardized Johnson $R$ and $I$ magnitudes for 37 Eri were determined by S. Cortesi at Specola Solare Ticinese to be $R = 4.70 \pm 0.02$ mag and $I = 4.30 \pm 0.02$ mag, while Cutispoto derived standardized Johnson $UBV$ and Kron-Cousins $RI$ magnitudes for HD 25852 of $U = 9.66 \pm 0.02$ mag, $B = 8.849 \pm 0.005$ mag, $V = 7.839 \pm 0.005$ mag, $R = 7.034 \pm 0.008$ mag, and $I = 6.183 \pm 0.10$ mag. The Kron-Cousins $RI$ photometry has been transformed to the Johnson $RI$ system with the equations in Bessell (1979) to combine them with the other observations.

The APT began nightly observations of HD 26337 on JD 2,447,072. Its schedule, however, was revised for nine nights between 1987 December 21 and 30, the time of the spectroscopic observations. During this time, only three program stars were on the master observing list: HD 26337, HD 80715, and 11 LMi. Beginning with 1988 January 1 the APT reverted to its routine operation program and continued to observe HD 26337 on a nightly basis until JD 2,447,232.

Figure 4 is a plot of the new $V$-band photometry versus Julian date from the observatories listed in Table 1. Only data with internal uncertainties of less than 0.02 mag are plotted.

TABLE 5

A. Ca II H AND K EMISSION LINE SURFACE FLUXES (ergs cm$^{-2}$ s$^{-1}$) FROM HD 26337

| Number | $\phi_{rot}$ | log $\mathcal{F}$(H) | log $\mathcal{F}$(K) | log $\mathcal{F}'$(H) | log $\mathcal{F}'$(K) |
|---|---|---|---|---|---|
| 1..... | 0.034 | 6.66 | 6.72 | 6.66 | 6.71 |
| 2..... | 0.145 | 6.705 | 6.797 | 6.692 | 6.786 |
| 3..... | 0.215 | 6.699 | 6.801 | 6.686 | 6.790 |
| 4..... | 0.510 | 6.58 | 6.54 | 6.58 | 6.52 |
| Mean values for radiative losses | | | | 6.66 | 6.71 |

B. FLUXES FROM OTHER G5 IV STARS

| Star | log $\mathcal{F}'$(H) | log $\mathcal{F}'$(K) | Source |
|---|---|---|---|
| χ Eri | ... | 5.88 | 1 |
| δ Pav | ... | 5.45 | 1 |
| 94 Aqr | ... | 5.88 | 1 |
| μ Her A | 5.14 | 5.23 | 2 |
| HD 31738 | 6.69 | 6.75 | 2 |
| HD 12545 | 6.65 | 6.70 | 2 |

REFERENCES.—(1) Pasquini, Pallavicini, and Pakull 1988. (2) Strassmeier *et al.* 1990.

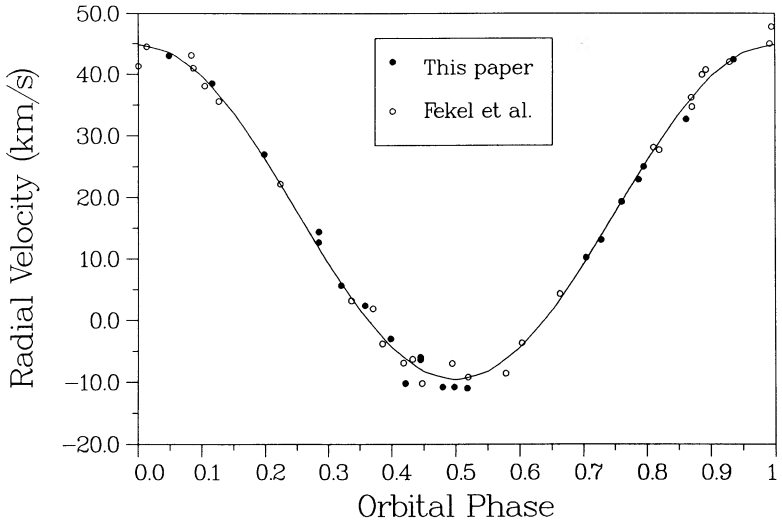


FIG. 2.—Observations and computed radial velocity curve. Dots are the new measures; circles are those from Fekel *et al.* (1987). Phase is computed from a time of maximum positive velocity.

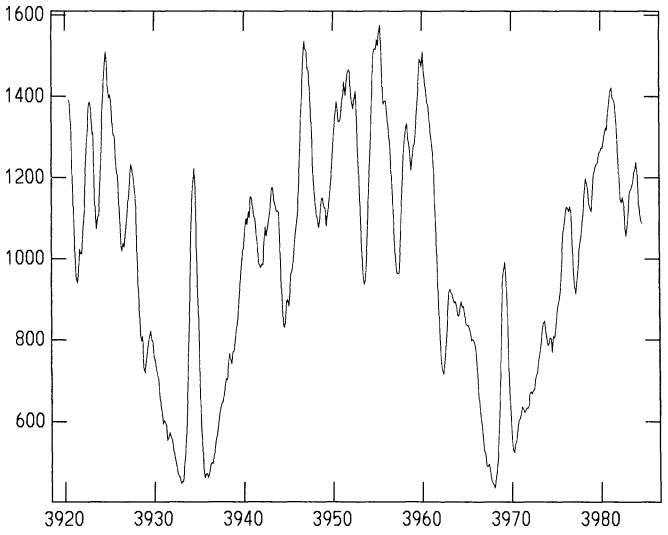


FIG. 3.—Ca II H and K region of HD 26337 showing the strong emission lines. Horizontal axis is in angstroms and vertical axis is in analog-to-digital units.

The choice of this 0.02 mag value as the cutoff was discussed in detail by Hall, Kirkpatrick, and Seufert (1986). Notice that observations on even-numbered nights trace out light curves with a beat period of 84 days when compared to odd-numbered nights. The time of the spectroscopic observations is indicated as a horizontal arrow. A more detailed discussion of *all* photometry is presented elsewhere (Hooten *et al.* 1989).

All observations in this paper have been phased together with the mean rotation period of $1.945 \pm 0.005$ days reported by Hall *et al.* (1987) and an initial epoch corresponding to a time of minimum light given in Fekel *et al.* (1982):

$$\mathrm{HJD} = 2{,}444{,}635.65 + 1.945E \, .$$

### *b) The Spot Temperature*

Vogt (1981) presented a method which decouples geometric effects (spot area and distribution on the surface) from the effective temperature information by using standardized $V$ and $R$ photometry and the Barnes-Evans relation (Barnes, Evans, and Moffett 1978). We have used this method to derive a first estimation of the spot temperature.

A Fourier fit, allowing for cos $\theta$ and cos $2\theta$ terms, of the 1988.13 *VRI* light curves gave amplitudes of $\Delta m_V = 0.067 \pm 0.016$ mag, $\Delta m_R = 0.059 \pm 0.013$ mag, and $\Delta m_I = 0.053 \pm 0.010$ mag, which leads to $(V-R)_{\mathrm{star}} - (V-R)_{\mathrm{spot}} = -0.78 \pm 0.05$ mag. Using the $V-R$ versus $T_{\mathrm{eff}}$ slope of Johnson (1966), this color difference implies a temperature difference (star minus spot) of $1860 \pm 400$ K and, with $T_{\mathrm{star}} = 5460$ K from the G5 subgiant classification, one gets an effective spot temperature of $3600 \pm 400$ K.

The final spot temperature is then derived within the modeling process by simultaneously adjusting the amplitude of the $V-I$ color curve while the $V$ light curve shape and amplitude is maintained. The observed $V-I$ amplitude of $0.014 \pm 0.006$ mag has rather large error bars, so that the spot temperature obtained is also rather uncertain but nevertheless agreed (formally) to within 20 K with the temperature from the $V$ and $R$ amplitudes. We therefore adopted $3600 \pm 400$ K as the effective spot temperature, which corresponds roughly to a spectral type M1 $\pm$ 0.5 for the spot.

### *c) The Unspotted Brightness Level*

Investigation of all available photometry from the past 9 years (which will be discussed in § VII) showed that HD 26337 was brightest in 1987.82 with $V_0 = 6.960 \pm 0.004$ mag, approximately the same magnitude observed in 1980.11 ($V_0 = 6.963$ mag) by Lloyd-Evans and Koen (1987). Thus, we have adopted 6.960 mag as the "least spotted" $V$ magnitude for the first modeling trial. The 1987–1988 season *VI* light curves were then fitted with theoretical light curves generated with a spot modeling computer program developed by Strassmeier (1988). The adopted spot model served as the starting input for the Doppler imaging program using only the calcium line at 6439 Å. It became clear immediately that the light curve solution did not agree with the Doppler imaging solution: the line profiles are filled in at all phases, while the light curve solution had three distinct spot areas at the equator and no spot above the circumpolar latitude. Reversing the modeling process, that is, solving first for the line profile variations and then computing a theoretical light curve with this spot model, showed that the observed mean $V$ light level was fainter by 0.057 mag. We then adjusted the "least spotted" $V$ magnitudes by this amount to obtain the "true" immaculate light level of $V_{0,\mathrm{max}} = 6.903$ mag. This is an important result for stellar spot modeling: although we had 9 consecutive years of $V$-band photometry, we still

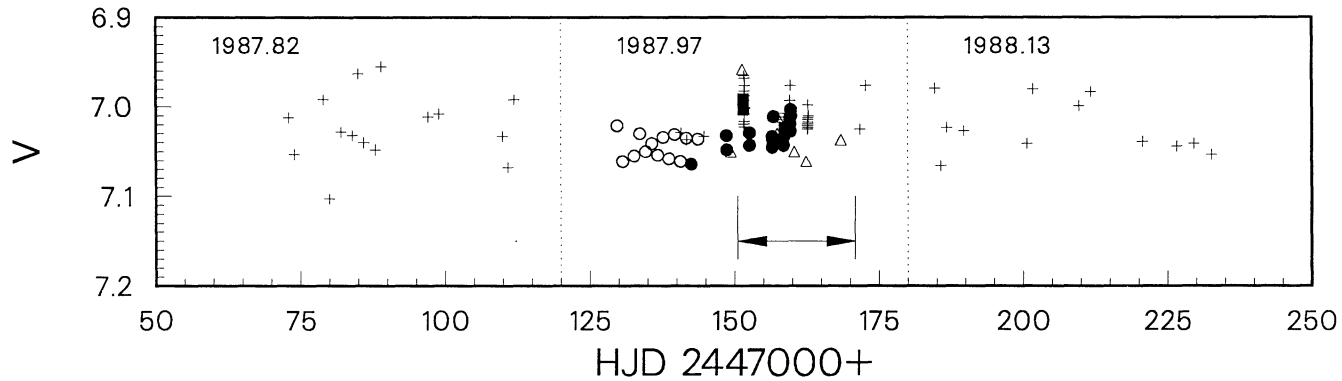


FIG. 4.—Julian Date plot of the 1987–1988 observing season $V$ photometry containing data from the Vanderbilt APT (+), Barksdale (●), Cutispoto (○), Goméz *et al.* (△), and Soder (■). Time of spectroscopic observations is marked by the horizontal arrow. Complete data set has been divided into three approximately equal groups according to midtimes of 1987.82, 1987.97, and 1988.13. Notice the fact that even-numbered nights and odd-numbered nights are shifted by approximately 0.5 phase due to the nearly 2-day period (the beat period is 84 days).

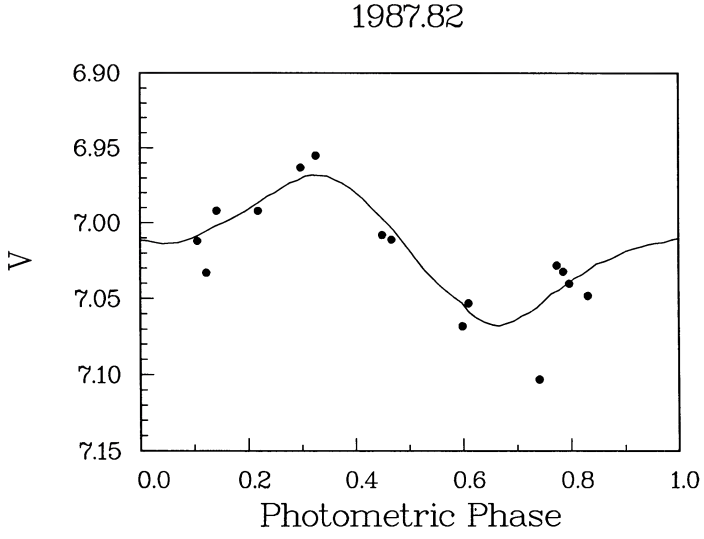


FIG. 5a

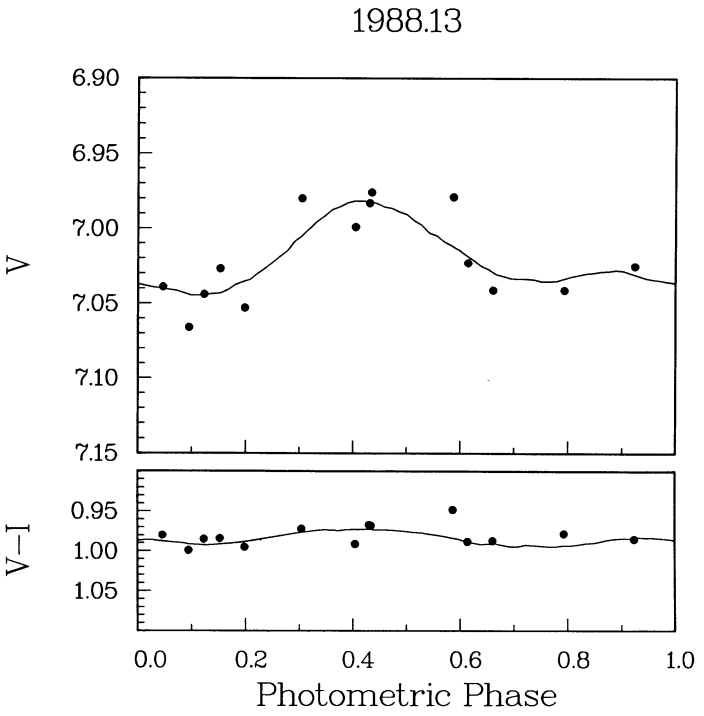


FIG. 5c

FIG. 5.—$V$ and $V-I$ light and color curves from the 1987–1988 observing season for (*a*) 1987.82, (*b*) 1987.97, and (*c*) 1988.13, respectively. The 1987.82 and 1988.13 data have been obtained with the Vanderbilt APT only, while the different symbols in the 1987.97 light curve belong to the observers indicated in the legend to Fig. 4. The lines are fits with theroetical spot models. Of particular interest is the 1987.97 light curve obtained partially simultaneously with the line profile observations (indicated as tick marks at the bottom of the upper panel). Because this light curve is a combination of data from a variety of observatories, we present two different techniques of how data were combined (method 1 in the upper panel and method 2 in the lower panel; see text). Full line in the upper panel is an "eye" estimated spot model fit to data obtained during the first half of this data portion and does not represent a fit based on least squares. Dotted line is the solution from the 1988.13 light curve in (*c*).

underestimated the "unspotted" magnitude by an amount which changed the generated spot models considerably. In a photometric study of five BY Dra and RS CVn stars, Rodonó *et al.* (1986) noted that the unspotted magnitude of their

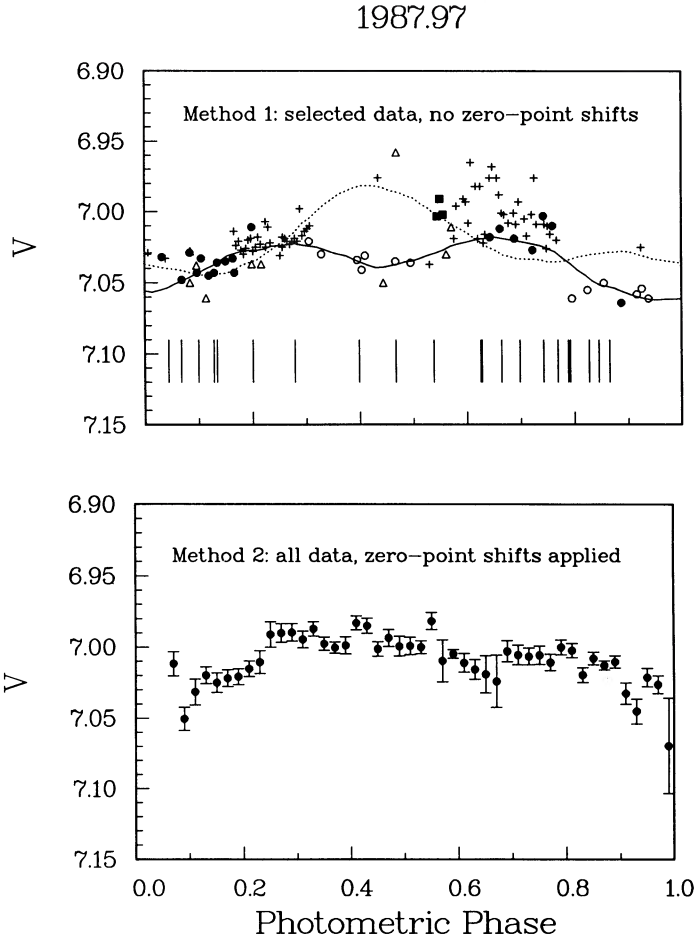


FIG. 5b

program stars was always brighter than the observed magnitude at light maximum. They anticipated that this could be due to either (*a*) high-latitude or nearly polar spots, (*b*) small nearly equatorial spots suitably distributed over a wide range of longitude, or (*c*) a uniform distribution of small spots over the stellar surface.

### *d) Spot Modeling*

Combining the value of the mass function (Table 2) and estimates of the upper and lower limit of the secondary's mass, Fekel *et al.* (1987) derived an inclination of $46° \pm 12°$, which has been adopted for our spot modeling throughout this paper.

The 1987–1988 season photometry displayed in Figure 4 has been divided into three consecutive data groups corresponding to midtimes of 1987.82, 1987.97, and 1988.13. In the following, we will discuss the modeling of the individual light curves.

#### i) *The 1987.82 V Light Curve*

Figure 5*a* shows the 1987.82 $V$ light curve along with the adopted spot model fit (Table 6). No $R$ and $I$ observations were available for this period. The light curve has one asymmetric minimum and is best fitted with a polar spot and two spots near the equator (Fig. 6*a*). We point out that light curve modeling does not allow one to extract useful information about a spot's latitude unless one already knows the spot area, the spot

TABLE 6

SPOT MODEL SOLUTIONS FOR THE 1987–1988 SEASON LIGHT CURVES

| SPOT PARAMETERS | DATE OF OBSERVATION | | |
|---|---|---|---|
| | 1987.82 | 1987.97[a] | 1988.13 |
| Number of spots | 3 | 4 | 3 |
| Spot A: | | | |
| Longitude | ... | 98°–118° | ... |
| Latitude | ... | 0°–27° | ... |
| Area[b] | ... | 1.26% | ... |
| Spot B: | | | |
| Longitude | 10°–50° | 320°–340° | 350°–15° |
| Latitude | 17°–40° | 0°–25° | 20°–40° |
| Area | 1.95% | 0.59% | 1.04% |
| Spot C: | | | |
| Longitude | 240°–260° | 226°–262° | 210°–240° |
| Latitude | 5°–30° | 7°–25° | 5°–27° |
| Area | 1.15% | 1.50% | 1.53% |
| Polar spot: | | | |
| Low latitude | 72° | 72° | 70° |
| Area | 2.45% | 3.01% | 3.01% |
| Total spotted area | 5.55% | 6.36% | 5.58% |
| Total $V$ amplitude (mag) | 0.095 | 0.043 | 0.069 |
| Total $I$ amplitude (mag) | ... | 0.033 | 0.055 |

NOTE.—Adopted system parameters: $V_{0,\max} = 6.903$ mag; $T_{\rm eff}$(star) = 5460 K; $T_{\rm eff}$(spot) = 3600 K; $u_V, u_R, u_I = 0.65, 0.50, 0.40$, $i = 46°$.

[a] Full line in Fig. 5*b*.

[b] In percents of the *total* surface of the star.

temperature, and the inclination of the star's rotation axis. Thus, for simplicity, we started the iterations by placing one end of the spot at the stellar equator. A Fourier analysis of the data with the 1.945 day rotation period gave a full $V$ amplitude of $0.075 \pm 0.018$ mag.

ii) *The 1987.97 VRI Light Curve*

Visual inspection of data from JD 2,447,120 through 2,447,180 in Figure 4 might tell us that the system underwent a rather rapid brightening of approximately 0.05 mag in $V$ between JD 2,447,149 and 2,447,151; that is, within *one* rotation cycle. Similar photometric behavior occurred earlier in 1985.7 (see § VII). However, the present data come from a variety of observatories which, when initially plotted against phase, exhibited large scatter and apparent systematic errors which were different from observatory to observatory. Since none of the observatories covered all phases, we propose two different methods for combining the photometry (Hooten *et al.* 1989): method 1 uses only data from observatories which have internal errors less than 0.02 mag and no apparent systematic zero point shifts. The resulting light curve is plotted in the upper panel of Figure 5*b*. Method 2 combines *all* data (except those which are grossly in error, say, 0.1 mag) and applies systematic corrections. The steps involved in determining these corrections were (1) average the observations of each observatory within Julian Date bins of width 0.007 days; (2) as a first approximation, consider the light curve to be of the form $l = A_0 + A_1 \cos \Theta + A_2 \cos 2\Theta$, where $A_0$, $A_1$, and $A_2$ are the Fourier coefficients and $\Theta$ is the photometric phase, and solve for the coefficients by means of least squares; (3) for each observatory, determine the shift (in magnitudes) which will make the average of the residuals from the curve be zero; (4) assign each observatory a weight given by $1/\sigma^2$, where $\sigma$ is the rms residual from the curve (after the shift has been applied); (5) divide the light curve into phase bins of width 0.02 phase, and calculate a weighted average of all observers in each phase bin; (6) assign a relative error, $(1/\Sigma\sigma^2)^{-1/2}$, to each phase bin. The resulting light curve is plotted along with the relative errors in the lower panel of Figure 5*b*. We cannot decide which method leads to the better result, but it is nevertheless worth discussing the light curves:

*First method.*—Data combined from observations made *before* JD 2,447,150 form the two minima at phase 0.45 and 0.95. Visual inspection shows the minimum at phase 0.95 rather asymmetric; i.e., not sinusoidal. The presence of an asymmetric minimum *and* a second distinct minimum cannot be fitted with a two-spot model; thus, a three spot model, in addition to the polar spot, has been adopted, and is plotted as a full line in the upper panel of Figure 5*b* and illustrated in Figure 6*b*. The steep decline of the light curve from phase 0.75 to 0.85 requires either a very cool spot or an unrealistically large spot elongated in latitude and could not be modeled with *one*, even practically black ($T_{\rm star} - T_{\rm spot} > 2000$ K), circular or quadratic spot. This supports the same findings of Doyle *et al.* (1988) for the large and steep photometric variations of II Peg in late 1986. Assuming the lower limit for the inclination ($i = 34°$) and a warmer spot ($T_{\rm spot} = 4200$ K), the computer program cannot fit this steep slope at all. Even a rectangular spot extending from $-40°$ to $+70°$ latitude and only 10° wide in longitude cannot reproduce the observations. On the other hand, if we assume the upper limit for the inclination ($i = 58°$) and $T_{\rm spot} = 4200$ K, a fit with an elongated triangularly shaped spot is possible. Its (estimated) sum of the O − C squares, moreover, is slighly larger than in the $i = 46°$ solution, so we believe that $T_{\rm spot} \sim 3600$ K and $i = 46°$ is actually a good choice and that the "real" inclination must be somewhere between 40° and 60°. It might be worthwhile to note also that we had to enlarge the polar spot by about 20% to keep down the total $V$ brightness level as compared to the previous observing season.

Data combined from observations *after* JD 2,447,150 show only one minimum at phase ~0.1 and a maximum at 0.5, the same phase were we have seen a minimum a few nights before. Comparison of tentatively obtained spot solutions before and after JD 2,447,150 reveals that spot A at phase ~0.45 fully disappeared within a time scale comparable to the rotation period and that spot B (at phase ~0.9) decreased its area at the same time by about 50%. While the coverage at the phases around 0.9 and 0.45 *after* JD 2,447,150 is rather poor, only three points from two different observers, thus calling into question the reality of these changes, it should be noted that the following light curve at 1988.13 (plotted as a dotted line in Fig. 5*b*, *upper panel*) shows maxima at the same phases and magnitude levels as seen in the 1987.97 light curve after JD 2,447,150.

*Second method.*—Figure 5*b* (*lower panel*) is a plot of the corrected $V$ magnitudes versus phase; the error bars were calculated by the method described above in step 6. Notice how tight the light curve became, showing only one minimum of approximately 0.03 mag at phase 0.1 and almost no variations between phases 0.2 through 0.9.

iii) *The 1988.13 VRI Light Curve*

Figure 5*c* is a plot of the $V$ and $V-I$ light and color curve for 1988.13 along with the spot model fit (Table 6). The two minima at phase 0.1 and 0.75 can be reproduced with a two-spot model and the same polar spot as in the second half of 1987.97. This is illustrated in Figure 6*c*. A Fourier analysis of

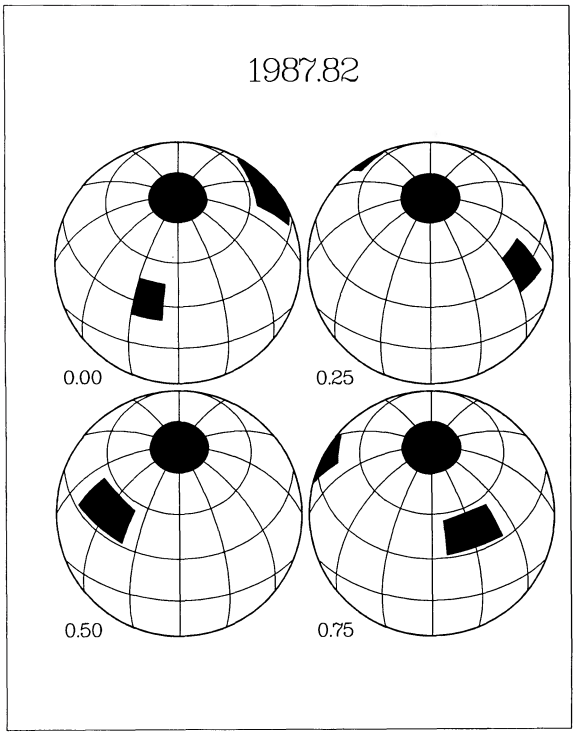


FIG. 6a

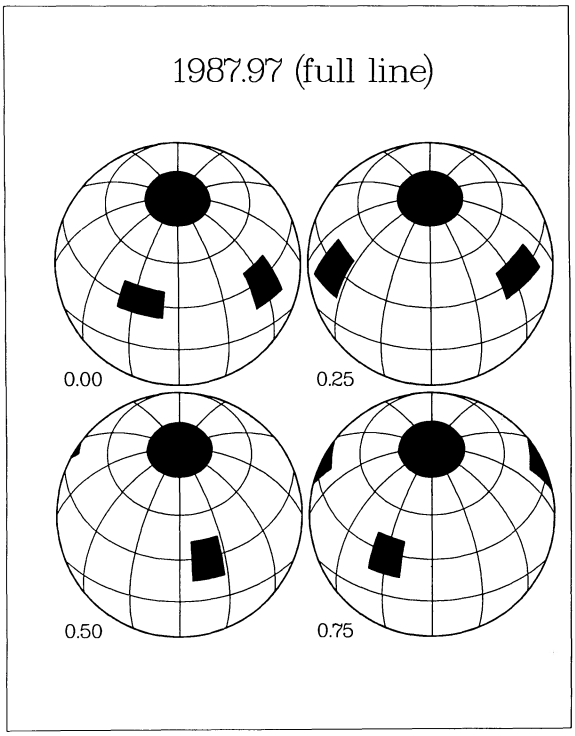


FIG. 6b

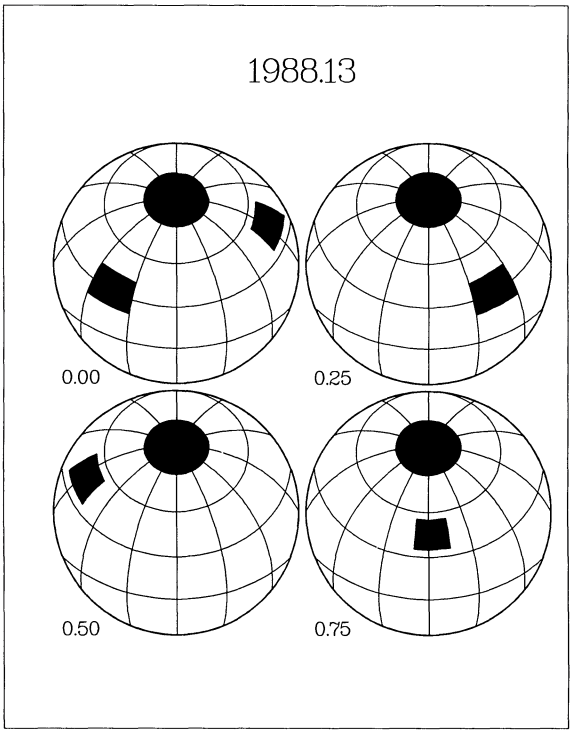


FIG. 6c

FIG. 6.—Spot models obtained from (*a*) the 1987.82 light curve, (*b*) the 1987.97 light curve before JD 2,447,150 (full line in Fig. 5*b*), and (*c*) the 1988.13 light curve.

the data gave $V$, $R$, and $I$ amplitudes of $0.067 \pm 0.016$, $0.059 \pm 0.013$, and $0.059 \pm 0.010$ mag, respectively.

## VI. DOPPLER IMAGING

### *a) The Observations*

A total of 21 high-resolution high S/N ratio spectra fairly well distributed over rotational phase were obtained at KPNO and NSO within 20 nights beginning at JD 2,447,150.6 (Table 2). The phased times of observation are plotted as tick marks in Figure 5*b* along with the simultaneous photometry. The spectra have been reduced in the standard fashion using the Image Reduction and Analysis Facility's (IRAF)[2] subpackage for CCD spectra (Pilachowski and Barnes 1987). A comparison of the spectra from the different telescope-spectrograph-detector combinations is shown in Figure 1.

### *b) Line Blending*

All of the observations included the Ca I line at 6439.08 Å and the Fe I line at 6430.85 Å (see Fig. 1); most of them also the Fe I line at 6411.66 Å. The Ca I and Fe I (6430 Å) lines are thought to be suitable for Doppler imaging (Vogt and Penrod 1983), but the Fe I 6430 line turned out to be problematic, particularly because it is blended due to rotational broadening with a nearby Fe II line at 6432.7 Å. It turned out that deblending this line is not a straightforward process. The simple reason is that the (broadened) Fe II feature is itself a blend with an unidentified line at 6433.45 Å (Pierce and Breckinridge 1973), and its mirrored red profile half cannot be used to deblend the Fe I line. This blend probably also affects the line profile variations at the line bottom, and a Doppler map from this line

[2] IRAF is distributed by National Optical Astronomy Observatories, which is operated by the Association of Universities for Research in Astronomy, Inc., under contract with the National Science Foundation.

might be false and misleading. We decided not to use Fe I λ6430 for the modeling procedure but to use it for comparison purposes and to plot the observations in Figure 8*b*. The same is also true for the Fe I λ6411.66 line (Fig. 8*c*), which is blended with another Fe I line at 6411.11 Å (equivalent width in μ Her ~40 mÅ). Moreover, several of the coudé feed observations did not include the 6411 Å region, so we did not include this line in the mapping process either.

Blending with very weak (mostly unknown) telluric water lines can also affect the line profile variations. Visual inspection of several spectra of the very narrow-lined stars μ Her (G5 IV), αCMi (F5 IV–V), and β Gem (KO III), taken at similar air masses and at the rest wavelengths plus/minus the radial velocity amplitude of HD 26337, did not reveal any significant telluric lines above the noise level. Therefore, no corrections have been applied to the line profiles.

### *c) Phase Smearing*

As a result of the short rotation period of 1.945 days, both the bumps in the line profile and the line itself will shift during the time of integration because of the changing radial velocity. The resulting profile is, therefore, phase smeared proportional to the integration time.

The coudé feed spectra sometimes needed an integration time of 90 minutes, while the McMath spectra required only 50–60 minutes to achieve the same S/N ratio (Table 2). A 90 (60) minute integration corresponds to 11° (8°) of spot motion in longitude on the stellar surface if the spot is at or near the central meridian. Formally, therefore, we will overestimate the spot's longitude extent by this upper limit, though this is not of great concern because 11° on the stellar surface is still within one resolution element ($\sim 7$ km s$^{-1}$) across the broadened line profile (full width $\sim 100$ km s$^{-1}$).

### *d) The Intrinsic Line Profile*

The Doppler imaging process requires knowledge of the intrinsic (Voigt) profile arising from the "quiet" photosphere of the star. In this paper, we approximate the intrinsic flux profile with the rotationally unbroadened lines of a standard star of the same spectral type and luminosity class. In particular, we used μ Her A, spectral classification G5 IV (Keenan 1983), $v \sin i = 1.2 \pm 1.0$ km s$^{-1}$, and radial-tangential macroturbulence $\zeta_{RT} = 4.5 \pm 0.4$ km s$^{-1}$ (Gray and Nagar 1985). A representative example of μ Her line profiles is shown in Figure 7. This approximation has several practical advantages: first, one does not need to know the instrumental profile(s); second, we can circumvent the computation of the specific intensity profiles from model atmospheres; and third, we do not need an assumption for the radial-tangential macroturbulence function. However, as Vogt (1988) noted, if the line-equivalent width is different in the spot than it is in the surrounding "quiet" photosphere, what actually will be modeled is a combination of surface brightness and line strength. The use of a standard star with the (assumed) uniform properties of the "quiet" photosphere of HD 26337 will therefore neglect possible spot versus photosphere differences in equivalent width. By using this technique, we assume implicitly that the shape and strength of the intrinsic line profile arising from the spot is the same as from the surrounding photosphere. This might be dangerous if the spot contributes a considerable amount of flux (Vogt, Penrod, and Hatzes 1987). The observed temperature difference (star minus spot) of 1860 K, however, means that the spots are very dark and contribute almost no flux.

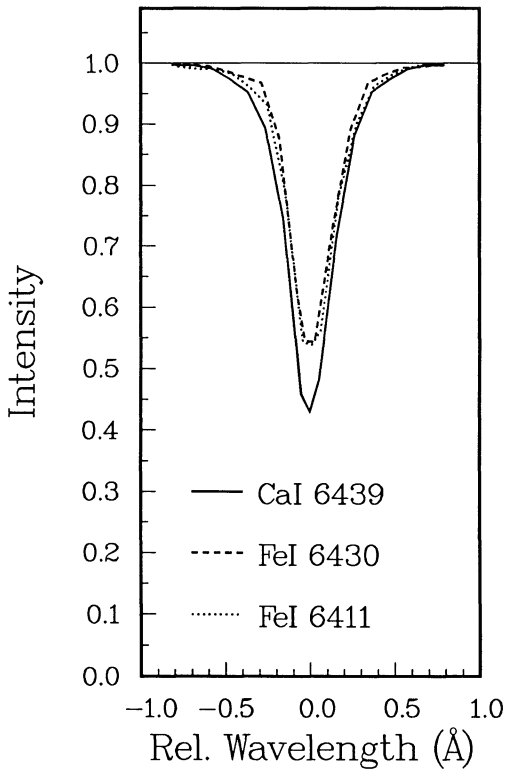


FIG. 7.—Examples of profiles of the Fe I lines at 6430 and 6411 Å, and the Ca I line at 6439 Å of μ Her A used to approximate the intrinsic line flux profile for HD 26337. These profiles were obtained with the "CF5, TI-3" configuration (Table 2).

### *e) Equivalent Width Measures*

The Fe I λ6411 line and the Ca I λ6439 line were measured by integration of the pixel intensities between the two pixels where the line reaches the continuum. For the Fe I λ6430 line

TABLE 7

EQUIVALENT WIDTHS OF PHOTOSPHERIC LINES

| NUMBER | $\phi_{rot}$ | EQUIVALENT WIDTH (mÅ) | | |
|---|---|---|---|---|
| | | Ca I λ6439.08 | Fe I λ6430.85 | Fe I λ6411.66 |
| 1..... | 0.044 | 204 | 160 | 136 |
| 2..... | 0.068 | 189 | 147 | 132 |
| 3..... | 0.100 | 198 | 147 | 125 |
| 4..... | 0.128 | 198 | 139 | 133 |
| 5..... | 0.134 | 194 | 147 | 136 |
| 6..... | 0.201 | 183 | 150 | 123 |
| 7..... | 0.279 | 171 | 141 | ... |
| 8..... | 0.399 | 187 | 138 | ... |
| 9..... | 0.467 | 205 | 150 | 133 |
| 10..... | 0.538 | 207 | 162 | 146 |
| 11..... | 0.625 | 201 | 153 | 135 |
| 12..... | 0.628 | 179 | 139 | ... |
| 13..... | 0.664 | 176 | 141 | ... |
| 14..... | 0.698 | 195 | 154 | 146 |
| 15..... | 0.742 | 195 | 147 | ... |
| 16..... | 0.756 | ... | ... | ... |
| 17..... | 0.769 | 185 | 133 | 126 |
| 18..... | 0.788 | 198 | 142 | ... |
| 19..... | 0.792 | 186 | 133 | 126 |
| 20..... | 0.816 | ... | ... | ... |
| 21..... | 0.827 | 191 | 139 | 129 |
| 22..... | 0.845 | 193 | 146 | 124 |
| 23..... | 0.865 | 195 | 140 | 116 |

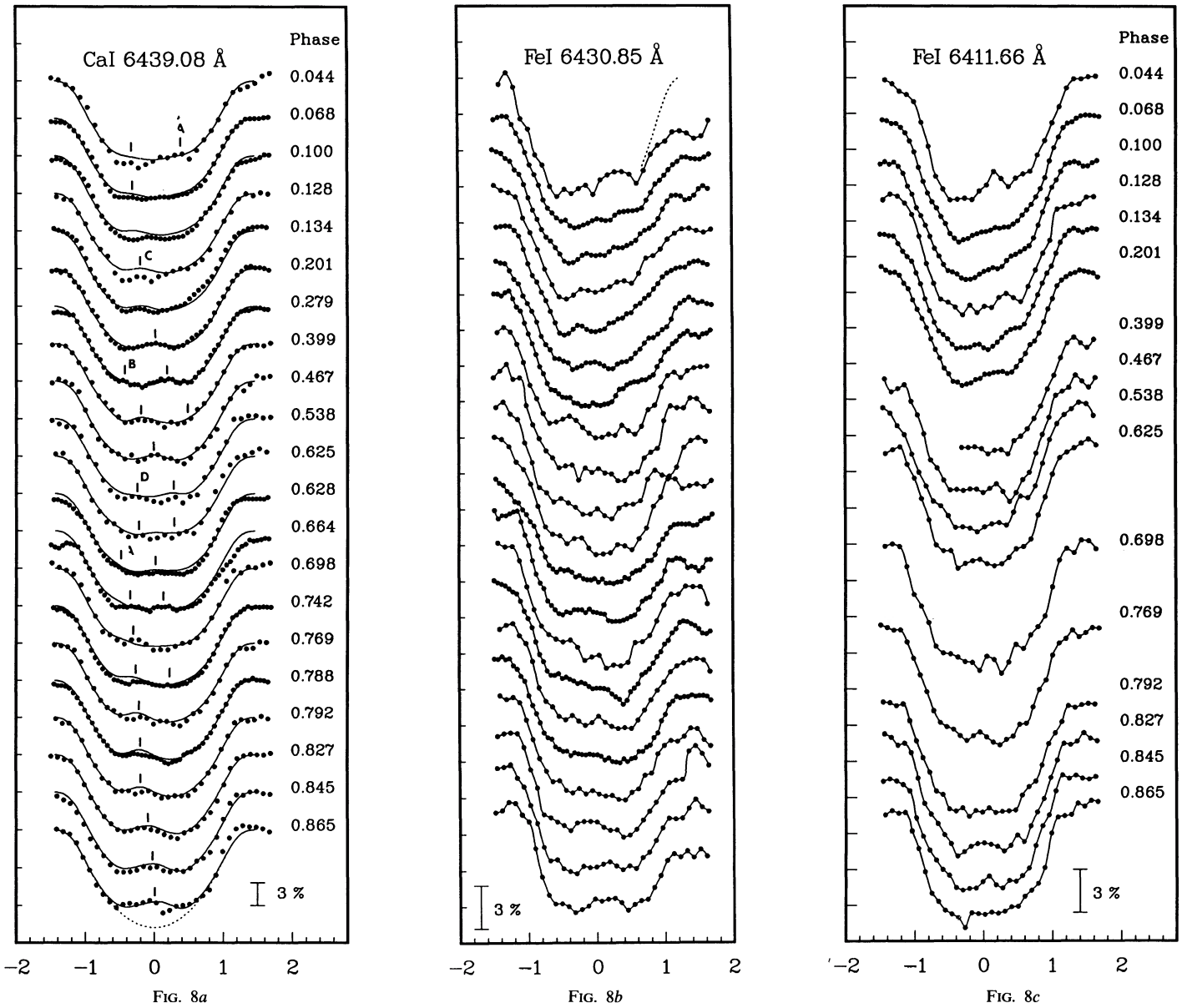


FIG. 8a FIG. 8b FIG. 8c

FIG. 8.—Line profile variations in the (*a*) Ca I 6439 Å line, (*b*) Fe I 6430, and (*c*) Fe I 6411 during 1987 December/1988 January. Observations are indicated by dots. Solid lines in the Ca I λ6439 panel are the theoretical profiles from the spot model. Also indicated are the profile bumps discussed in the text and identified in Fig. 9. Solid lines in the other panels are simple spline fits to the data. Phase represents the same photometric (=rotation) phase as used for the light curves. Some of the KPNO coudé feed spectra did not include the Fe I λ6411 line. Notice the permanently filled-in line cores, due presumably to a polar spot. This is particularly visible in the lower Ca I profile, where the dotted line indicates the theoretical profile without spots. Also note the distortion of the Fe I λ6430 line due to the Fe II line at 6432 Å (the dotted line is an approximation of the true location of the Fe I profile wing).

we removed the (approximated) Fe II blend by applying a subroutine available in the IRAF CCD spectra package which performs a nonlinear least-squares Gaussian fit to the line and the blend and removes the latter. Table 7 lists the measured equivalent widths for the three lines considered for the Doppler imaging analysis. The estimated total error for one measure is approximately 10%, although the systematic error from observations made one after the other during the same night is less than 3%.

### *f*) *Deriving the Spot Map*

The first step was to find out if the variations in the three line profiles show the same pattern. From careful inspection of Figure 8, it was clear that the profile variations agree qualitatively but that there is no guarantee that small details are real if they do not show up in all three lines. Altogether we see three major bumps (designated A, B, and C), and one weaker bump (designated D) in all three lines, and we reject smaller detail as noise. Although the strength of the bumps is larger in the Fe I λ6430 line than in the calcium line, the Ca I profiles are more homogeneous and seem to be more reliable.

The second step was to obtain a good initial guess of the spot distribution. This was easily done: we simply used the model from the light curve solution (illustrated in Fig. 6*b*, one polar spot and three spots near the equator). Not unexpectedly, the fit obtained was qualitatively quite good, except

that all four bumps traveled much too fast across the line profiles. Thus, the spots were positioned at incorrectly low latitudes. Our best solution after seven iterations implies spots at very high latitudes. Actually, with the exception of spot D, they can be viewed as part of one irregular *polar* spot. A test run with a larger inclination of the rotation axis ($i = 55°$) resulted in basically the same map with just slightly enlarged spots.

The third step was to compare the Doppler imaging solution with the photometry. Now we used the Doppler map as the input model for the light curve synthesis program, generated a theoretical $V$ light curve, and compared it with the simultaneous photometric observations. Again, the agreement was *qualitatively* good in the sense that the Doppler solution correctly reproduced the longitude of the photometric minima and maxima if compared with the light curve in Figure 5*b*, method 1. Quantitatively, the amplitude was too small by a factor of 2 when compared with the first half of the 1987.97 data set, and too small by a factor of 3 when compared with the second half. The agreement is much better if we consider the light curve in Figure 5*b*, method 2, the theoretical amplitude being only 0.01 mag smaller; i.e., approximately 50% of the observed amplitude. I would like to point out that our simultaneous photometry could not cover all phases because of the almost exactly 2 day rotation period; thus, the comparison of photometric and spectroscopic observations necessarily included nonsimultaneous photometry.

At this point, we must again deal with the rapid photometric variations seen around JD 2,447,150 (§ IV). First, the spectroscopic observations started on that very same night and hence may be affected by these variations, if they exist. This would explain our inability to obtain a better fit to parts of the profiles at early phases (Fig. 8*a*). Second, as mentioned before, the incomplete phase coverage of the 1987.97 light curve (if only *exactly* simultaneous photometric observations are used, as indicated in Fig. 4) would actually allow a much smaller amplitude than that seen when observations from a larger time span are phased together. This leads to the possibility that the amplitude *was* small.

### *g) Discussion of the Spot Map*

As can be seen from Figure 8*a*, the fit of the theoretical line profiles is in most cases good to about 1% except for the line profiles at phases 0.044, 0.100, and 0.128, where the sum of the O − C's is more like 2%. The solution presented is the best we could find, keeping in mind that we used two different telescopes/spectrographs and a variety of CCD detectors. Despite all problems encountered, the existence of a polar or nearly polar spot on HD 26337 (Fig. 9) is well determined and agrees with earlier Doppler maps of other spotted stars: the RS CVn binary HR 1099 (Vogt and Penrod 1983; Vogt 1988), and the FK Com star HD 199178 (Vogt 1988).

The fact that the Doppler imaging technique produced spots at quite different latitudes compared to the light curve modeling technique is no surprise. With "real" photometric data, say, external precision of 0.01 mag or slightly better, there is no way to extract good latitude information from a light curve.

Our spot map in Figure 9 with smaller spots (A, B, C, and D) close to or even touching the big polar spot also supports the poleward migration scenario suspected for the starspots on HR 1099 and the eventual merging into the polar spot (Vogt 1988); this is quite opposite to the spot behavior on our Sun. In the following § VII, modeling of 9 consecutive years of photometry, we might find further evidence for this scenario.

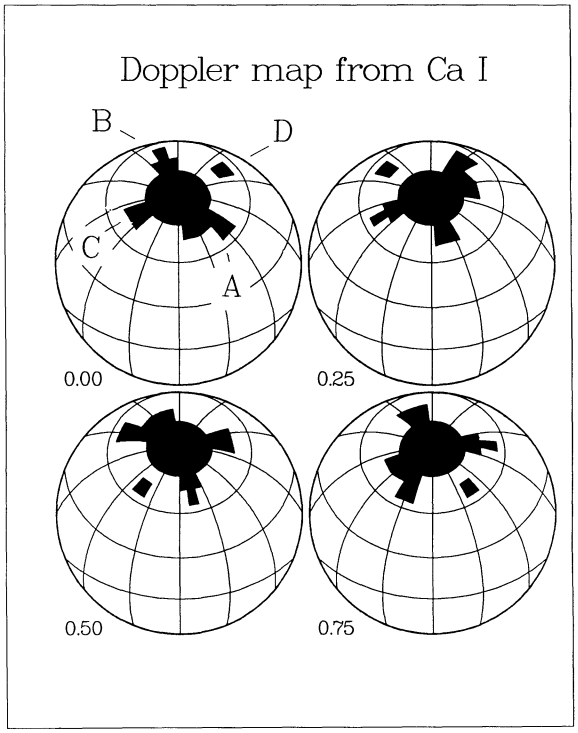


FIG. 9.—Spot map from the Doppler imaging process of the Ca I line profile variations. The presence of an asymmetric polar spot is obvious. The reality of details on the order of a resolution element ($\approx 10°$ on the stellar surface), however, should be considered with caution.

## VII. NINE YEARS OF PHOTOMETRY

### *a) The Data*

Table 8 is a summary of the available photometry found in the literature along with a new light curve obtained in 1987.12 and the 1987–1988 observing season photometry already described in § V. The table lists the separate light curves according to their respective midtimes, followed by the Julian Dates of the first and last observation, the number of data points (average of three integrations on the variable), the rotation cycles covered, the maximum $V$ brightness, and the source reference. The *IUE*-FES observations of Baliunas, Blair, and Guinan (1983), transformed to $V$ of the Johnson $BV$ system, have been shifted by 0.150 mag to align them with the simultaneous ground-based observations of Barksdale as reported in Hall *et al.* (1987).

### *b) Spot Modeling*

The availability of 23 $V$ light curves from the 1979–1980 observing season through the 1987–1988 season enables us to follow the spot activity throughout approximately 9 years. We have applied a multiple-spot-model computer program (Strassmeier 1988) with rectangularly shaped spots and the adopted system and spot parameters already described in § V (e.g., Table 6: "Adopted Parameters"). The polar spot has been used to adjust the maximum brightness level, $V_0$, of each individual light curve, while spots close to the equator are used to model the amplitude and shape of the light curves; thus, their respective size is somewhat model dependent, and care is

TABLE 8

TALLY OF ALL AVAILABLE PHOTOMETRY

| Data Group | Mean Epoch | HJD First last | $n$ | Rotation Cycles Covered | $V_0$ | Source |
|---|---|---|---|---|---|---|
| 1 ..... | 1979.77 | 244 4129 4183 | 10 | 28 | 6.988[a] | Lloyd-Evans and Koen 1987 |
| 2 ..... | 1980.01 | 244 4234 4253 | 15 | 10 | 6.996[a] | Lloyd-Evans and Koen 1987 |
| 3 ..... | 1980.11 | 244 4263 4298 | 15 | 18 | 6.963[a] | Lloyd-Evans and Koen 1987<br>Fekel *et al.* 1982 |
| 4 ..... | 1980.75 | 244 4499 4526 | 15 | 14 | 6.982 | Fekel *et al.* 1982 |
| 5 ..... | 1980.93 | 244 4550 4605 | 17 | 28 | 7.024[a] | Lloyd-Evans and Koen 1987<br>Fekel *et al.* 1982 |
| 5b..... | 1981.02 | 244 4614 | 1 | ... | (7.11) | Fekel, Moffett, and Henry 1986 |
| 6 ..... | 1981.11 | 244 4633 4660 | 9 | 14 | 6.980[a] | Lloyd-Evans and Koen 1987<br>Fekel *et al.* 1982 |
| 7 ..... | 1981.00 | 244 4520 4660 | 14 | 72 | ... | Bopp *et al.* 1983 |
| 8 ..... | 1981.91 | 244 4904 4874 | 10 | 36 | 7.081[a] | Lloyd-Evans and Koen 1987 |
| 9 ..... | 1982.92 | 244 5260 5350 | 7 | 46 | 7.06 | Hall *et al.* 1987 |
| 10 ..... | 1983.10 | 244 5304 5400 | 4 | 49 | (7.20) | Baliunas, Blair, and Guinan 1983 |
| 11 ..... | 1984.04 | 244 5700 5732 | 22 | 16 | 7.078 | Strassmeier *et al.* 1989 |
| 12 ..... | 1984.12 | 244 5732 5757 | 16 | 13 | 7.090 | Strassmeier *et al.* 1989 |
| 13 ..... | 1984.79 | 244 5972 6002 | 19 | 16 | 7.038 | Strassmeier *et al.* 1989 |
| 14 ..... | 1984.86 | 244 6002 6026 | 22 | 12 | 7.006 | Strassmeier *et al.* 1989 |
| 15 ..... | 1984.94 | 244 6031 6055 | 10 | 12 | 7.048 | Strassmeier *et al.* 1989 |
| 16 ..... | 1985.04 | 244 6065 6098 | 14 | 17 | 7.048 | Strassmeier *et al.* 1989 |
| 17 ..... | 1985.13 | 244 6098 6126 | 14 | 14 | 7.058 | Strassmeier *et al.* 1989 |
| 18 ..... | 1985.70 | 244 6307 6334 | 17 | 14 | 7.054 | Strassmeier *et al.* 1989 |
| 19 ..... | 1985.76 | 244 7334 6353 | 17 | 10 | (7.07) | Strassmeier *et al.* 1989 |
| 20 ..... | 1985.85 | 244 6353 6396 | 38 | 22 | 7.070 | Strassmeier *et al.* 1989 |
| 20b..... | 1985.85 | 244 6373 | 1 | ... | (7.18) | Reglero *et al.* 1987 |
| 21 ..... | 1987.12 | 244 6821 6867 | 10 | 23 | 7.015 | This paper |
| 22 ..... | 1987.82 | 244 7073 7112 | 15 | 20 | 6.960 | This paper |
| 23 ..... | 1987.97 | 244 7130 7172 | 109 | 21 | ... | This paper |
| 24 ..... | 1988.13 | 244 7185 7232 | 12 | 24 | 6.978 | This paper |

[a] Based on all-sky photometry.

necessary not to overinterpret these parameters. Actually, this fitting procedure will always produce the *upper* limit of the size of the polar spot and the *lower* limit of the size of the "equator" spots. This, however, does not affect the total spotted area. Consequently, we have plotted only the sum of the area of the "equator" spots in Figure 11. Another point of concern is the ambiguity of any derived information on the *latitudes* of the spots. To be consistent throughout the modeling procedure, we placed the spots always at the *same* latitude. For simplicity, the lower boundary of the rectangular spots remains fixed at the equator, and we call these spots A, B, and (sometimes) C. Finally, we need two more assumptions: first, all spots have the *same* temperature difference (photosphere minus spot), and second, this temperature does not vary with time.

With these assumptions in the back of our minds, the individual light curves were then fitted with three- or four-spot models (one permanent spot at the pole and two or three "equator" spots). The best fits are shown in Figures 10*a*–10*d* as dotted lines along with the observations and are listed in Table 9. No solutions were obtained for the 1979.77 light curve and the 1980.93 light curve (Fig. 10*a*) because of either poor phase coverage or significant variations within the covered time interval.

TABLE 9

SPOT MODEL SOLUTIONS FOR THE 1980–1987 PHOTOMETRY[a]

| MEAN EPOCH | $\Delta V_{min}$[b] (mag) | $\Delta V_{max}$[b] (mag) | SPOT LIMITS | | | TOTAL AREA[c] |
|---|---|---|---|---|---|---|
| | | | Longitude | Latitude | Area[c] | |
| 1979.77..... | 1.642 | 1.547 | ... | ... | ... | ... |
| 1980.01..... | 1.646 | 1.554 | P: 0–360 | 70 | 3.0 | 6.4 |
| | | | A: 160–190 | 0–15 | 1.1 | |
| | | | B: 65–100 | 0–25 | 2.1 | |
| | | | C: 265–275 | 0–10 | 0.2 | |
| 1980.11..... | 1.665 | 1.527 | P: 0–360 | 75 | 1.7 | 6.6 |
| | | | A: 180–210 | 0–25 | 1.8 | |
| | | | B: 115–140 | 0–45 | 2.5 | |
| | | | C: 315–330 | 0–20 | 0.7 | |
| 1980.75..... | 1.688 | 1.57: | P: 0–360 | 72 | 2.4 | 8.5 |
| | | | A: 85–110 | 0–20 | 1.2 | |
| | | | B: 20–53 | 0–35 | 2.6 | |
| | | | C: 280–315 | 0–27 | 2.2 | |
| 1980.93..... | 1.688 | 1.57: | ... | ... | ... | ... |
| 1981.00..... | 1.760 | 1.595 | P: 0–360 | 66 | 4.3 | 9.6 |
| | | | A: 170–190 | 0–15 | 0.7 | |
| | | | B: 350–15 | 0–21 | 1.3 | |
| | | | C: 260–302 | 0–35 | 3.3 | |
| 1981.11..... | 1.743 | 1.548 | P: 0–360 | 70 | 3.0 | 8.7 |
| | | | A: 195–235 | 0–35 | 3.2 | |
| | | | B: 320–345 | 0–15 | 0.9 | |
| | | | C: 275–295 | 0–35 | 1.6 | |
| 1981.91..... | 1.677 | 1.648 | P: 0–360 | 61 | 6.3 | 7.0 |
| | | | A: 130–150 | 0–10 | 0.5 | |
| | | | B: 50–63 | 0–10 | 0.3 | |
| 1982.92..... | 1.693 | 1.630 | P: 0–360 | 62 | 5.8 | 7.8 |
| | | | A: 190–205 | 0–17 | 0.6 | |
| | | | B: 255–280 | 0–23 | 1.4 | |
| 1983.10..... | 1.723 | 1.623 | P: 0–360 | 62 | 5.8 | 7.8 |
| | | | A: 190–205 | 0–17 | 0.6 | |
| | | | B: 255–280 | 0–23 | 1.4 | |
| 1984.04..... | 1.735 | 1.637 | P: 0–360 | 62 | 5.8 | 9.9 |
| | | | A: 205–235 | 0–30 | 2.1 | |
| | | | B: 50–60 | 0–10 | 0.2 | |
| | | | C: 320–345 | 0–30 | 1.7 | |
| 1984.12..... | 1.746 | 1.662 | P: 0–360 | 61 | 6.3 | 9.5 |
| | | | A: 125–140 | 0–20 | 0.7 | |
| | | | B: 10–25 | 0–27 | 0.9 | |
| | | | C: 285–315 | 0–23 | 1.6 | |
| 1984.79..... | 1.788 | 1.600 | P: 0–360 | 65 | 4.7 | 10.2 |
| | | | A: 242–270 | 0–17 | 1.1 | |
| | | | B: 65–80 | 0–15 | 0.5 | |
| | | | C: 327–17 | 0–34 | 3.8 | |
| 1984.86..... | 1.740 | 1.579 | P: 0–360 | 67 | 4.0 | 8.7 |
| | | | A: 290–325 | 0–35 | 2.8 | |
| | | | B: 25–50 | 0–35 | 2.0 | |
| 1984.94..... | 1.741 | 1.618 | P: 0–360 | 63 | 5.4 | 8.4 |
| | | | A: 265–295 | 0–35 | 2.4 | |
| | | | B: 30–45 | 0–17 | 0.6 | |
| 1985.03..... | 1.741 | 1.618 | P: 0–360 | 63 | 5.4 | 8.4 |
| | | | A: 265–295 | 0–35 | 2.4 | |
| | | | B: 30–45 | 0–17 | 0.6 | |
| 1985.13..... | 1.821 | 1.618 | P: 0–360 | 63 | 5.4 | 10.3 |
| | | | A: 277–327 | 0–35 | 4.0 | |
| | | | B: 30–55 | 0–15 | 0.9 | |
| 1985.70..... | 1.843 | 1.631 | P: 0–360 | 62 | 5.8 | 10.0 |
| | | | A: 165–205 | 0–45 | 3.9 | |
| | | | B: 50–60 | 0–10 | 0.2 | |
| 1985.76..... | 1.727 | 1.630 | P: 0–360 | 62 | 5.8 | 8.4 |
| | | | A: 210–230 | 0–30 | 1.4 | |
| | | | B: 140–160 | 0–25 | 1.2 | |
| 1985.85..... | 1.711 | 1.632 | P: 0–360 | 62 | 5.8 | 8.8 |
| | | | A: 320–340 | 0–30 | 1.4 | |
| | | | B: 210–230 | 0–35 | 1.6 | |
| 1987.12..... | 1.669 | 1.580 | P: 0–360 | 67 | 4.0 | 7.1 |
| | | | A: 200–220 | 0–30 | 1.7 | |
| | | | B: 95–125 | 0–22 | 1.4 | |

[a] "P" in the "Longitude" column denotes the polar spot; "A," "B," "C" denote the equator spots. Note that, e.g., spot C in one observing season could be named spot B in the following season because it is quite arbitrary to decide whether the spots migrated to a new position or a new spot has been formed. For the polar spot, only the lower latitude limit is given.

[b] In the sense HD 26337 minus 37 Eri.

[c] In percents of the *total* surface of the star.

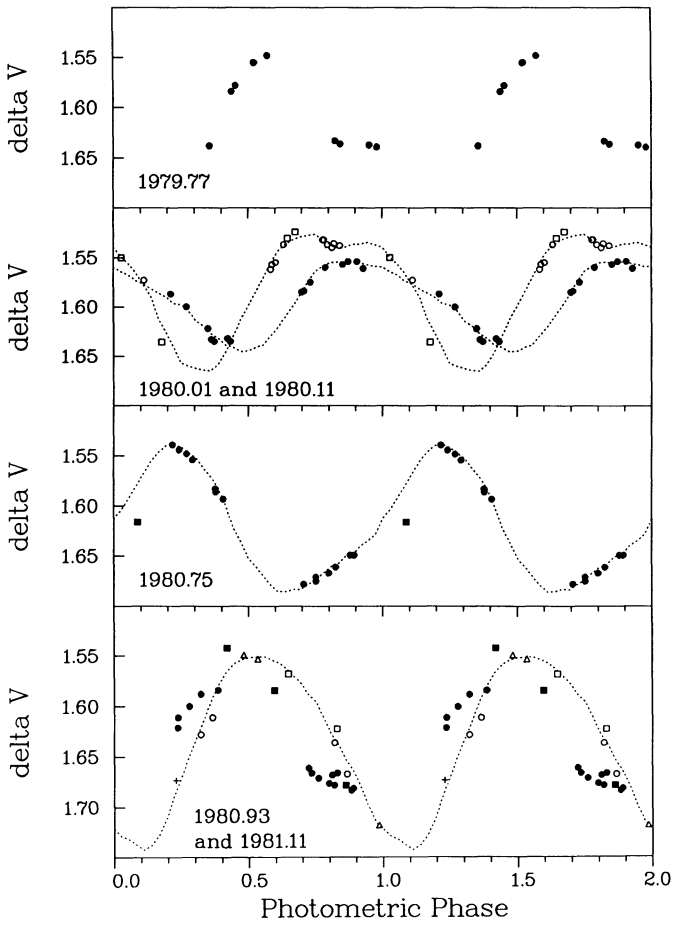


FIG. 10*a*

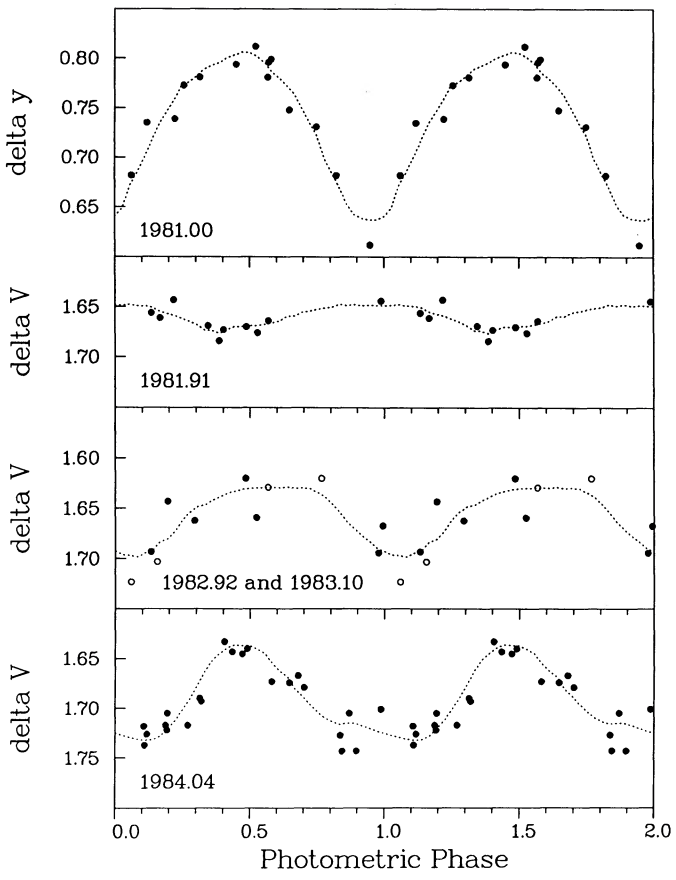


FIG. 10*b*

FIG. 10.—(*a*)–(*d*) Johnson *V*- and Strömgren *y*-band light curves of HD 26337 from 1979 through 1987. Different symbols within a subplot correspond generally to different observers, while "open" and "filled" symbols also indicate different data groups (Table 8): filled symbols precede epoch and open symbols follow (the single " + " in the "1980.93 and 1981.11" subplot belongs to data group 5*b* in Table 8). Notice the rapid light curve variation in the subplot labeled "1985.70 and 1985.76" starting with the marked observation (*arrow*) at JD 2,446,334. See text for discussion. For light curves later than the last one in (*d*), see Fig. 5 and § V in the text.

### *c) Discussion of the Modeling Results*

Visual inspection of the 1985.70 and 1985.76 light curves in Figure 10*d* reveals a significant change of the light curve minimum, which implies spot variations on a time scale of approximately one rotation cycle. Because of the 2-day rotation period and the nightly mode of observations, that is, a single observation each night at very much the same time, we can follow this change in time steps of two nights or one rotation cycle. In other words, the spacing of the data points in the mentioned light curves around phase 0.2 is one rotation cycle. The one marked point (arrow in Fig. 10*d*) at phase $\sim 0.15$ and $\Delta V \sim 1.75$ mag was the first point in the "1985.76" data set at JD 2,446,334, while the points at earlier phases were obtained on consecutive nights *preceding* JD 2,446,334 and the points at later phases were obtained on consecutive nights *following* JD 2,446,334. Thus the change took place at JD 2,446,334 on a time scale of one or two rotation cycles; that is, the same time scale as the similar phenomenon (spot area decreasing) seen in the 1987.97 light curve described in § V*d*. Similar variations, though not as rapid, seem to be common for HD 26337. Monthly variations can be seen in the "1980.01 and 1980.11" and "1980.93 and 1981.11" panels in Figure 10*a*, and even faster, say 25 days, in the late 1984 data in Figure 10*c*. Other times, e.g., in the "1984.94 and 1985.04" panel in Figure 10*c*, the light curve remains stable for 1 month or maybe $1\frac{1}{2}$ months (or roughly 20 rotation cycles).

The results of the spot modeling procedure are plotted versus time in Figure 11 (and listed in Table 9), where the bars in the upper panel indicate the full *V* amplitude and the mean light level; the middle panel shows the spot distribution in longitude and their longitude sizes; and the lower panel plots the spot area of the combined "equatorial" spots A, B, and C (shaded area labeled "A + B + C"), the polar spot (*dashed line*), and the sum of the two, i.e., the total spotted area (*full line*). The following features are evident in the three panels of Figure 11.

1. There is a secular trend in the mean *V* light level. So far, the pattern has not repeated; hence, any spot cycle similar to the 11 yr sunspot cycle, if it exists, appears to be longer than the baseline of our data, which is approximately 8–9 yr. It is important to keep in mind that the *V* amplitude alone cannot be used to account for the degree of spottedness simply because a smaller amplitude can sometimes mean more spots; e.g., the solution of the 1981.92 light curve with an amplitude of only 0.03 mag had 10% *more* spots on the star than the 1980.11 light with an amplitude of 0.14 mag.

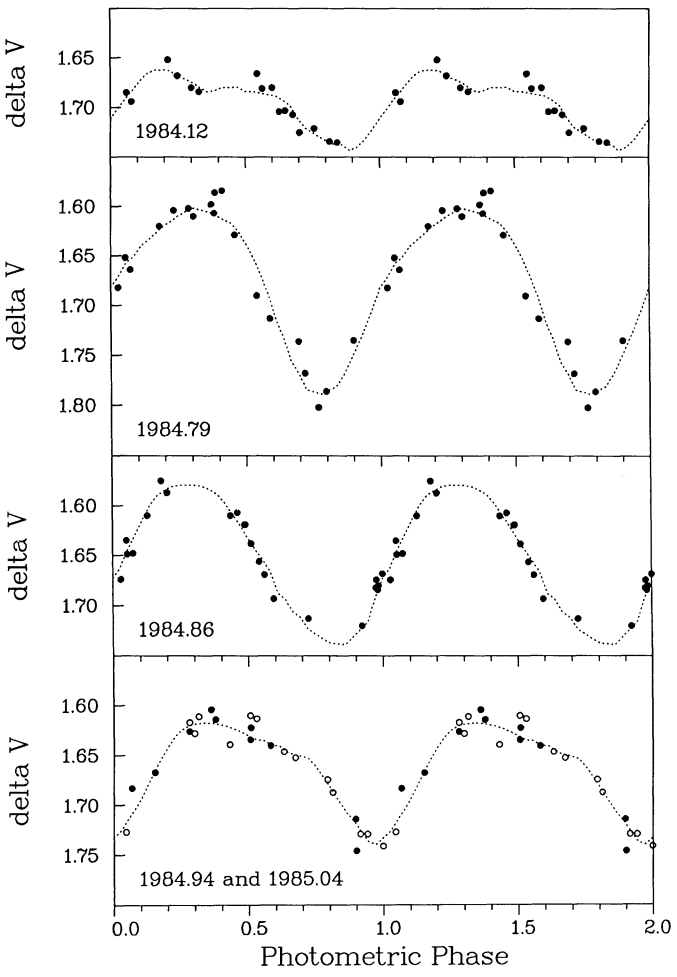


FIG. 10c

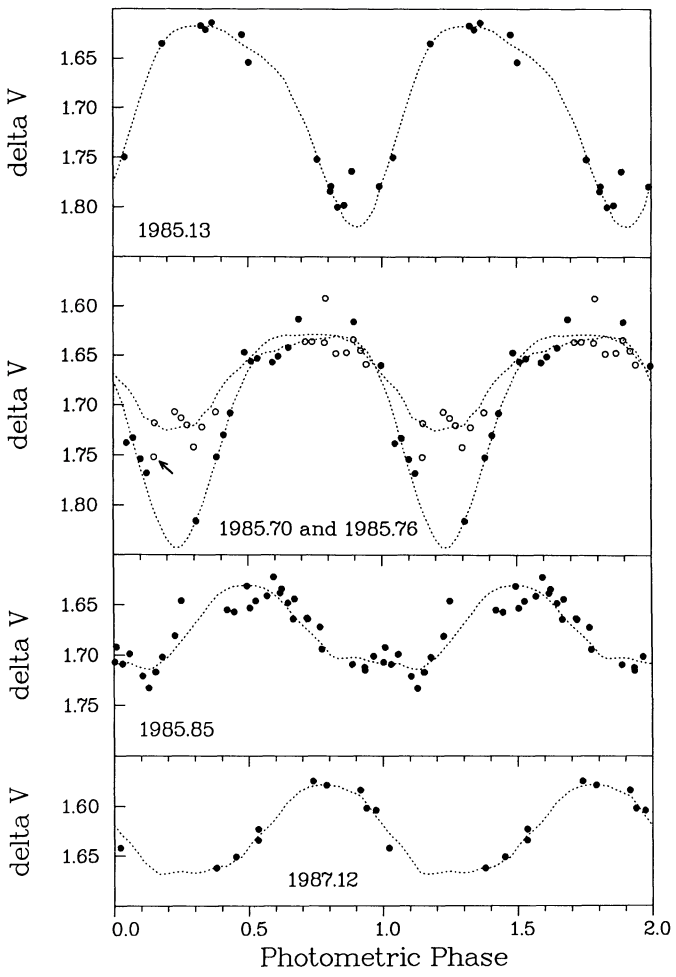


FIG. 10d

2. There seems to be no "preferential longitude" or "sector structure" (Eaton and Hall 1979) of the spotted regions on HD 26337, as has been suspected for other RS CVn stars; e.g., HK Lac (Oláh, Gesztelyi, and Holl 1987), V711 Tau (Bartolini *et al.* 1983), and RS CVn (Eaton and Hall 1979). Periodogram analysis by Hall *et al.* (1987) yielded season-to-season variations in the photometric period of $\sim 1\%$ which are presumably due to latitude and/or longitude changes of the starspot regions. Their mean value from 6 yr of photometry can be regarded as a good measure of the star's rotation period. By phasing our data with this value, we have already taken out the spot's "migration" due to the beat period between the orbital period and the rotation period. Consequently, the longitudes of the spots are in a coordinate system fixed to the star's rotation, and there is no obviously recognizable systematic pattern in the longitude versus time plot in Figure 11.

3. We observe very rapid spot variability which might indicate unexpectedly short spot lifetimes, say, less than 1 yr, probably only a few months. This is in contrast to the 20 yr lifetime of the spot on RS CVn (Blanco, Catalano, and Marilli 1983) and the 17 yr lifetime for the two spots on HK Lac (Oláh *et al.* 1986).

4. The total spotted area appears to change systematically with time but is interrupted by apparently non periodic, rapid changes of the area of one particular spot described earlier. The size of the "equator" spots changes proportional to the light curve amplitude while the polar spot, and thus the total spotted area, depends on the value chosen for the unspotted magnitude. As a matter of fact, by assuming the brightest observed light level as the unspotted magnitude and using only the photometric data, we would have been forced to introduce either a band of spots, as Bopp and Noah (1980) did for II Peg, or a polar spot in order to keep up with the low light level around 1984–1985. This supports further the existence of a polar spot, simply because a band of spots (below the circumpolar latitude) cannot explain the observed "filling" of the line profile *cores* (see § VI*f*).

The longitude positions of spots are sometimes significantly different between consecutive light curves closely spaced in time. The observations cannot tell us conclusively whether we are seeing the same spot at different longitudes or seeing a newly formed spot. This is especially problematic when comparing different observing seasons and is somewhat arbitrary. Nevertheless, if we use only light curves obtained within the same observing season, we can put some constraints on the most likely explanation for the spot motion: differential rotation. From the longitude versus time plot in Figure 11 (numerical values in Table 9), we can measure the motion of the spots in longitude, yielding $\Delta\omega$'s in the range $-3\overset{\circ}{.}0$ through $+1\overset{\circ}{.}7$ per day. The individual values are plotted in the histogram in Figure 12, where negative $\Delta\omega$ means faster rotation than at the corotation latitude and positive $\Delta\omega$ slower rota-

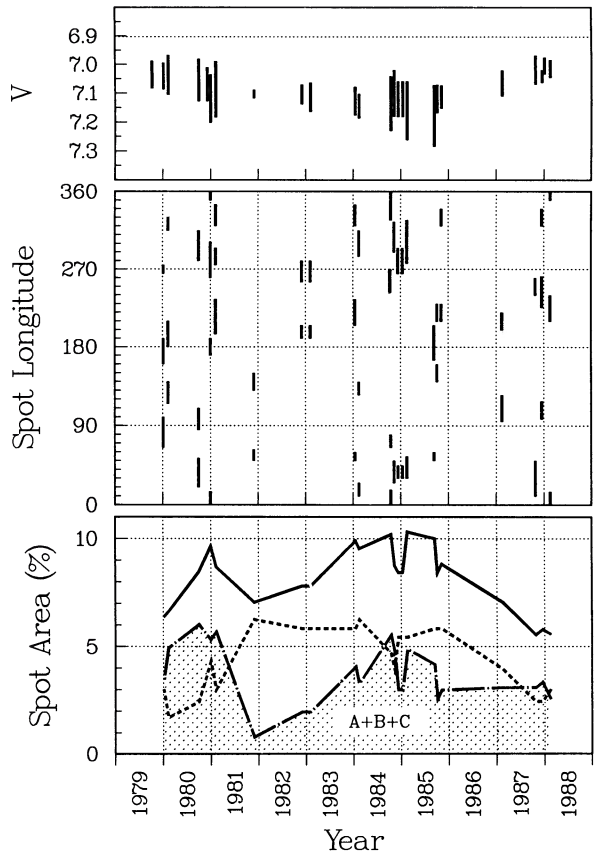


FIG. 11.—Long-term spot behavior. *Upper panel:* variation of the *V*-light level and amplitude. Dotted line indicates the unspotted magnitude. *Middle panel:* longitude position and size of the spots in a coordinate system fixed on the rotating star. Indicated are only the "equatorial" spots (up to three) as discussed in the text. Longitude of the spots is apparently randomly distributed and no "preferred longitude" can be seen in the data. *Lower panel:* spotted area as a percentage of the entire stellar surface. Solid line is the total spotted area. Dashed line is the area of the polar spot, and shaded part is the sum of the "equatorial" spots A, B, and C.

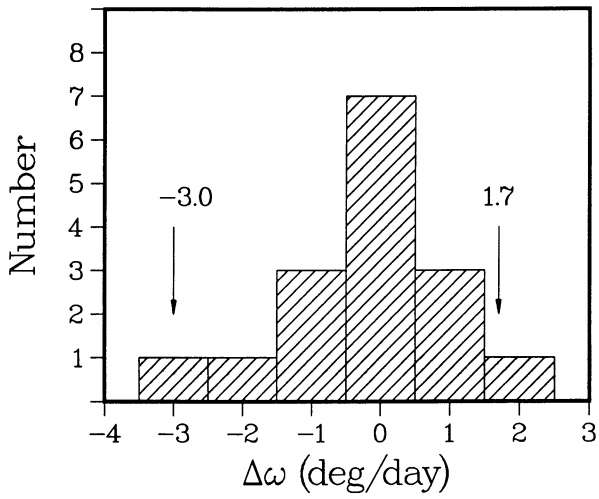


FIG. 12.—Distribution of measured longitude motions $\Delta\omega$ of spots A, B, and C (Table 9) with respect to the corotation latitude ($\Delta\omega = 0$). The smallest and largest value of $\Delta\omega$ indicate the lower and the upper latitude limit where spots occur. Since the inclination of the rotation axis is approximately 45°, the lower latitude limit is very likely the equator.

tion. The different values of $\Delta\omega$ can be understood if spots occur above or below the corotation latitude. If interpreted in the context of solar-like differential rotation, the maximum and minimum value of $\Delta\omega$ correspond to an upper and lower latitude limit, repectively. Since $i \approx 45°$, we observe primarily regions above the equator, and the lower latitude limit might be identical with the equator. The upper latitude limit must be very close to the pole, because our Doppler map showed a polar spot. The range of $\Delta\omega$ observed (4°.7 per day), normalized to the mean rotation period, yields $(\Delta\omega/\omega)_{\rm HD\ 26337} = 0.0254$. This implies a drift smaller by approximately a factor of 10 when compared to the solar value ($\omega_\odot$ [equator] $- \omega_\odot$ [latitude = 75°] = 3°.5 per day; Snodgrass 1983) and $(\Delta\omega/\omega)_\odot = 0.2467$, but is consistent with other stellar determinations (Rodonó 1986).

## VIII. CONCLUDING REMARKS

To conclude, we emphasize the existence of a cool polar spot on HD 26337. The photometry indicates that this polar spot is rather long-lived, persisting at least the 9 years for which we had photometry. The polar spot contributes only insignificantly to the light curve amplitude but it is crucial for the overall brightness of the system. At the other extreme, we also found evidence for extremely rapid light curve shape variations on a time scale of only one or two rotation cycles. These changes could be modeled by rapidly decreasing a spot area. Recently, Neff (1989) observed similar light curve variation of HD 26337 in 1988 September on a time scale of only one rotation cycle using the FES on board the *IUE* satellite. His observations covered two consecutive complete rotation cycles.

The most accurate parameter from light curve modeling is the stellar longitude of a spot. Returning to Figure 11, we emphasize the point that the longitude variations, when interpreted in the context of differential rotation, indicate spot migration approximately a factor of 10 smaller than on the Sun. We might understand some phenomena seen on HD 26337, such as the existence of a long-lived polar spot and short lived "equator" spots with very small migration rates, with the existence of a poleward meridional plasma flow in the convection zone of the stars, a phenomenon not unlike solar meridional flows. While this flow is trying to push the magnetic flux tubes toward higher latitudes, the differential rotation is trying to move them toward lower latitudes, causing the short lifetime and small migration rates. Moreover, this allows some spots to drift to the pole if they are formed at high latitudes, where differential rotation has little influence. However, much more observation is necessary to turn speculations into a well-established starspot hypothesis.

I am grateful to the referee, Steve Vogt, for his helpful suggestions which led to an improvement of this paper. I would also like to thank my colleague, Frank Fekel, for sharing valuable observing time with me on the KPNO coudé feed telescope and for numerous discussions concerning the spectroscopic data. Special thanks go to all the amateur astronomers who participated in this observing compaign and to G. Cutispoto for communicating his data prior to publication. It is also a pleasure to acknowledge the help of B. W. Bopp, who contributed two spectra simultaneous to the other spectroscopic observations. This paper has benefited from discussions and readings by S. S. Vogt and D. S. Hall. R. Wehrse and P. Noah deserve commendation for sending me their ver-

sions of the ATLAS stellar atmosphere program. Finally, I wish to acknowledge the financial support of the Austrian Bundesministerium für Wissenschaft und Forschung (Fulbright scholarship) and of the American Astronomical Society (Henri Chrétien Award). In addtion, this project was partially supported by NASA grant NAG 8–111.

REFERENCES

Baliunas, S. L., Blair, W. P., and Guinan, E. F. 1983, *Inf. Bull. Var. Stars*, No. 2323.
Barker, E. S., Evans, D. S., and Laing, J. D. 1967, *Royal Obs. Bull.*, No. 130.
Barnes, T. G., Evans, D. S., and Moffett, T. J. 1978, *M.N.R.A.S.*, **183**, 285.
Bartolini, C., *et al.* 1983, *Astr. Ap.*, **117**, 149.
Bessell, M. S. 1979, *Pub. A.S.P.*, **91**, 589.
Bidelman, W. P., and MacConnell, D. J. 1973, *A.J.*, **78**, 687.
Blanco, C., Catalano, S., and Marilli, E. 1983, in *IAU Colloquium 71, Activity in Red Dwarf Stars*, ed. M. Rodonó and P. Byrne (Dordrecht: Reidel), p. 387.
Bopp, B. W., Africano, J. L., Stencel, R. E., Noah, P. V., and Klimke, A. 1983, *Ap. J.*, **275**, 691.
Bopp, B. W., and Noah, P. V. 1980, *Pub. A.S.P.*, **92**, 717.
Boyd, L. J., Genet, R. M., and Hall, D. S. 1984, *Comm. Internat. Amateur Professional Photoelectric Photometry*, No. 15, p. 20.
Busso, M., Scaltriti, F., Persi, P., Ferrari-Toniolo, M., and Origlia, L. 1988, *M.N.R.A.S.*, **234**, 445.
Doyle, J. G., Butler, C. J., Morrison, L. V., and Gibbs, P. 1988, *Astr. Ap.*, **192**, 275.
Eaton, J. A., and Hall, D. S. 1979, *Ap. J.*, **227**, 907.
Fekel, F. C., Hall, D. S., Henry, G. W., Landis, H. J., and Renner, T. R. 1982, *Inf. Bull. Var. Stars*, No. 2110.
Fekel, F. C., Moffett, T. J., and Henry, G. W. 1986, *Ap. J. Suppl.*, **60**, 551.
Fekel, F. C., Quigley, R., Gillies, K., and Africano, J. L. 1987, *A.J.*, **94**, 726.
Gray, D. F., and Nagar, P. 1985, *Ap. J.*, **298**, 756.
Hall, D. S., Kirkpatrick, J. D., and Seufert, E. R. 1986, *Comm. Internat. Amateur Professional Photelectric Photometry*, No. 25, p. 32.
Hall, D. S., Osborn, S. A. G., Seufert, E. R., Boyd, L. J., Genet, R. M., and Fried, R. E. 1987, *A.J.*, **94**, 723.
Hooten, J. T., *et al.* 1989, *Ap. Space Sci.*, **155**, 45.
Johnson, H. L. 1966, *Ann. Rev. Astr. Ap.*, **4**, 193.
Keenan, P. C. 1983, *Bull. Inf. Centre de Donées Stellaires*, No. 24, p. 19.
Linsky, J. L., Worden, S. P., McClintock, W., and Robertson, R. M. 1979, *Ap. J. Suppl.*, **41**, 47.
Lloyd-Evans, T., and Koen, M. C. J. 1987, *South Africa Astr. Obs. Circ.*, **11**, 21.
Lucy, L. B., and Sweeney, M. A. 1971, *A.J.*, **76**, 544.
Mutel, R. L., and Lestrade, J. F. 1985, *A.J.*, **90**, 493.
Neff, J. E. 1989, private communication.
Nicolet, B. 1978, *Astr. Ap. Suppl.*, **34**, 1.
Oláh, K., *et al.* 1986, *Ap. Letters*, **25**, 133.
Oláh, K., Gesztelyi, L., and Holl, A. 1987, in *Proc. 10th European Regional Astr. Meeting of the IAU*, ed. P. Harmanec (*Pub. Czech. Acad. Sci.*, No. 70, p. 95).
Pasquini, L., Pallavicini, R., and Pakull, M. 1988, *Astr. Ap.*, **191**, 253.
Pierce, A. K., and Breckinridge, J. B. 1973, *Kitt Peak Nat. Obs. Contr.*, No. 559.
Pilachowski, C., and Barnes, J. 1987, *IRAF Reduction of Coudé/CCD Spectra*, (Tucson: NOAO/KPNO).
Reglero, V., Giménez, A., de Castro, E., and Fernandez-Figueroa, M. J. 1987, *Astr. Ap. Suppl.*, **71**, 421.
Rodonó, M. 1986, in *4th Cambridge Workshop on Cool Stars, Stellar Systems, and the Sun*, ed. M. Zeilek and D. M. Gibson (Heidelberg: Springer), p. 475.
Rodonó, M., *et al.* 1986, *Astr. Ap.*, **165**, 135.
Slee, O. B., Stewart, R. T., Nelson, G. J., Wright, A. E., Dulk, G. A., Bastian, T. S., and McKean, M. 1988, *Ap. Letters Comm.*, **27**, 247.
Snodgrass, H. P. 1983, *Ap. J.*, **270**, 288.
Strassmeier, K. G. 1987, *Inf. Bull. Var. Stars.*, No. 3049.
———. 1988, *Ap. Space Sci.*, **140**, 223.
Strassmeier, K. G., Fekel, F. C., Bopp, B. W., Dempsey, R. C., and Henry, G. W. 1990, *Ap. J. Suppl.*, in press.
Strassmeier, K. G., Hall, D. S., Boyd, L. J., and Genet, R. M. 1989, *Ap. J. Suppl.*, **68**, 141.
Vogt, S. S. 1981, *Ap. J.*, **250**, 327.
———. 1988, in *IAU Symposium 132, The Impact of Very High S/N Spectroscopy on Stellar Physics*, ed. G. Cayrel de Strobel and M. Spite (Dordrecht: Kluwer), p. 253.
Vogt, S. S., and Penrod, G. D. 1983, *Pub. A.S.P.*, **95**, 565.
Vogt, S. S., Penrod, G. D., and Hatzes, A. P. 1987, *Ap. J.*, **321**, 496.
Willmarth, D. W., and Abt, H. A. 1985, in *IAU Colloquium 88, Stellar Radial Velocities*, ed. A. G. D. Philip and D. W. Latham (Schenectady: Davis), p. 99.

KLAUS G. STRASSMEIER: Department of Physics and Astronomy, Vanderbilt University, Nashville, TN 37235